Meddelelser om Grønland

Mineralogy of the Werner Bjerge alkaline complex, East Greenland

C. Kent Brooks, John Engell, Lotte Melchior Larsen and Asger Ken Pedersen

Geoscience
7 · 1982

Meddelelser om Grønland

The series *Meddelelser om Grønland* undertook to publish results from all fields of research in Greenland. It has now been split into three separate series:
Geoscience
Bioscience
Man & Society

The series should be registered as *Meddelelser om Grønland, Geoscience (Bioscience, Man & Society)* followed by the number of the paper. Example: *Meddr Grønland, Geosci.* 1, 1979.

The new series are issued by Kommissionen for videnskabelige Undersøgelser i Grønland (The Commission for Scientific Research in Greenland).

Correspondence
All correspondence and manuscripts should be sent to:

The Secretary
Kommissionen for videnskabelige Undersøgelser i Grønland
Øster Voldgade 10
DK-1350 Copenhagen K.

Questions concerning subscription to any or all of the series should be directed to the agent.

Agent
Nyt Nordisk Forlag – Arnold Busck A/S, Købmagergade 49, DK-1150 Copenhagen K. Tlf. +45.1.111103.

Meddelelser om Grønland, Geoscience

Meddelelser om Grønland, Geoscience invites papers that contribute significantly to studies in Greenland within any of the fields of geoscience (physical geography, oceanography, glaciology, general geology, sedimentology, mineralogy, petrology, palaeontology, stratigraphy, tectonics, geophysics, geochemistry). Papers primarily concerned with other areas in the Arctic or Atlantic region may be accepted, if the work actually covers Greenland or is of direct importance to continued research in Greenland. Papers dealing with environmental problems and other borderline studies may be referred to either *Geoscience* or *Bioscience,* according to emphasis and editorial policy.

Editor
T. C. R. Pulvertaft, Institute of General Geology, Øster Voldgade 10, DK-1350 Copenhagen K. Tlf. +45.1. 112232. Telegr. Unigeol.

Instructions to authors. – See page 3 of cover.

Mineralogy of the Werner Bjerge alkaline complex, East Greenland

C. Kent Brooks, John Engell, Lotte Melchior Larsen and Asger Ken Pedersen

MEDDELELSER OM GRØNLAND, GEOSCIENCE 7 · 1982

Table of Contents

Accepted 09-07-1981
ISSN 0106-1046
ISBN 87-17-02961-9
Printed in Denmark by AiO Print as, Odense

Mineralogy of the Werner Bjerge alkaline complex, East Greenland

C. KENT BROOKS, JOHN ENGELL, LOTTE MELCHIOR LARSEN and ASGER KEN PEDERSEN

Brooks, C. K., Engell, J., Larsen, L. M. & Pedersen, A. K. 1982. Mineralogy of the Werner Bjerge alkaline complex, East Greenland. – Meddr Grønland, Geosci. 7: 35 pp. Copenhagen 1982-06-28.

The Tertiary Werner Bjerge complex is divided into a basic complex, a northern complex and a nepheline syenite complex. The basic complex consists of cumulate rocks (ranging from ultramafic to gabbros) containing plagioclase, clinopyroxene, olivine and titanomagnetite with intercumulus kaersutite or biotite and subsolidus amphiboles and sheet silicates. Similar cumulates but containing cumulus kaersutite occur as inclusions in dykes associated with the nearby Theresabjerg intrusion and have been included in the study. The northern complex includes a wide range of felsic rock types of which two granites have been examined. In the nepheline syenite complex the rock types investigated include foyaites, a tinguaite, and quartz-bearing pegmatite. The main minerals in these rocks are alkali feldspar, nepheline, sodalite, alkali pyroxene, alkali amphibole and biotite together with a wide range of minor and accessory phases.

Clinopyroxenes vary from diopsides and salites in the basic rocks to aegirine-augites and acmites in the more evolved types, which are unusually MnO-rich. Titan-aegirines occur in the pegmatite.

The amphibole in the basic rocks is kaersutite; in the granite it is manganoan richterite, and in the nepheline syenite complex the amphiboles vary from hastingsitic hornblende through katophorite to manganoan arfvedsonite. The pegmatite contains unique Li-arfvedsonites. Minor late-stage calcic amphiboles occur in the basic rocks.

Sheet silicates include micas and secondary mixed layer types, chlorite and talc. Primary micas of the basic complex are titaniferous biotites and in the nepheline syenites are Mn-rich biotites, while the pegmatite contains the rare Li-mica, taeniolite.

Feldspars range from bytownite in the basic rocks to mainly alkali feldspar in the nepheline syenites which is often optically homogeneous and strongly potassic. Analyses of feldspathoids and zeolites are also presented.

The oxides of the evolved rocks are also MnO-rich and pyrophanite has been encountered in both the granite and the nepheline syenites. Other Mn-rich phases are also present, such as Mn-pectolite and kupletskite (the Mn analogue of astrophyllite). Data have also been acquired for a wide range of accessory phases including (additionally) sulphides (pyrrhotite, pyrite and sphalerite), apatite, sphene, titanian garnets, narsarsukite, pyrochlore, calcite, chevkinite and several unidentified zirconosilicates from the nepheline syenites.

It is concluded that the geochemical coherence between the various rock units of the intrusion suggests a comagmatic origin for these, while the close similarities between the mineralogies of the Kangerdlugssuaq and Werner Bjerge alkaline complexes suggest a similar origin.

C. K. Brooks, Institute of Petrology, University of Copenhagen, Øster Voldgade 10, DK-1350 Copenhagen.

J. Engell, Institute of Industrial Mineralogy, Technical University of Denmark. Building 204, DK-2800 Lyngby.

L. M. Larsen, Geological Survey of Greenland, Øster Voldgade 10, DK-1350 Copenhagen.

A. K. Pedersen, Geological Museum, University of Copenhagen, Øster Voldgade 5–7, DK-1350 Copenhagen.

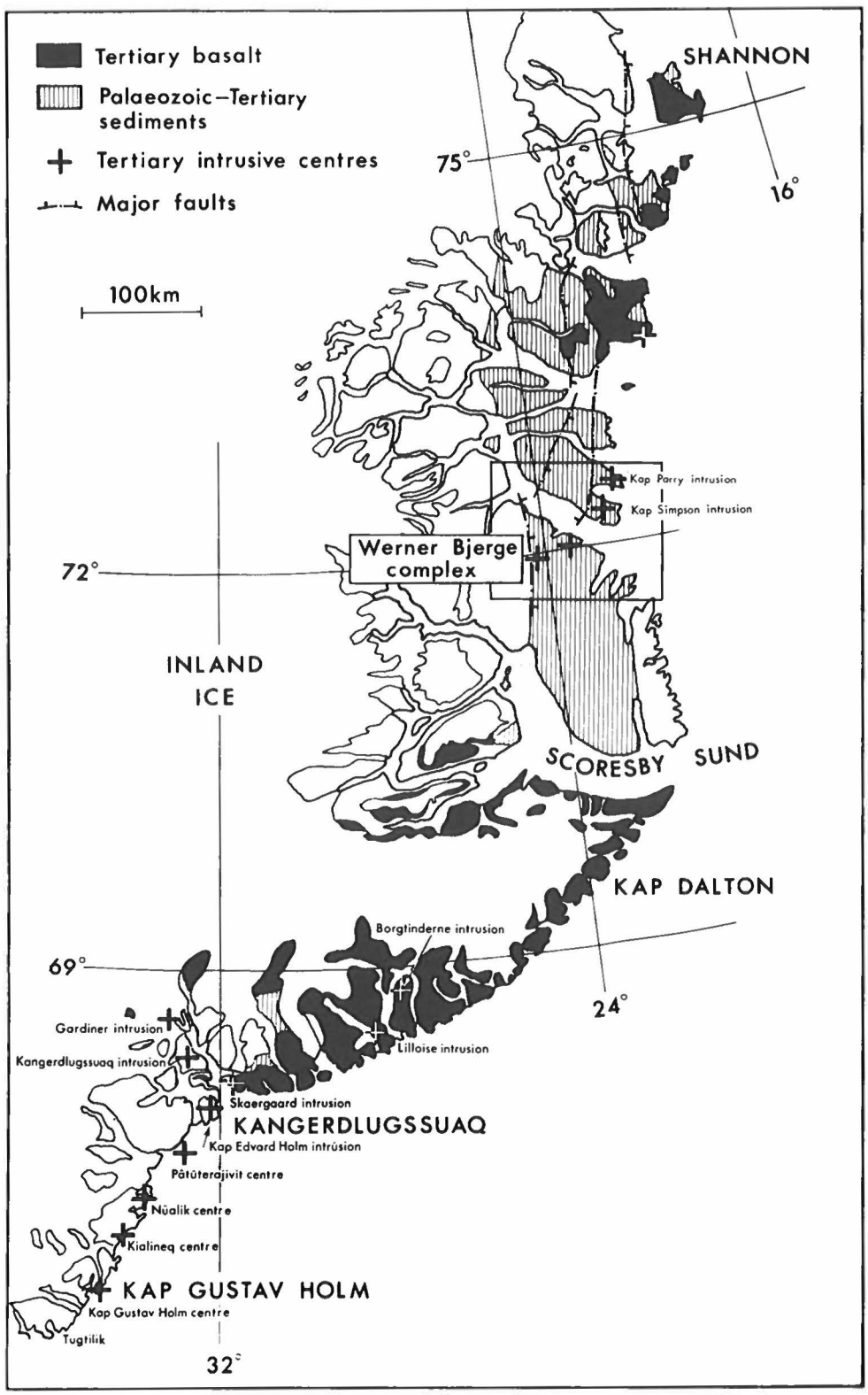

Fig. 1. The central part of East Greenland showing the distribution of Tertiary igneous rocks. The area shown in Fig. 2 is framed and the Werner Bjerge complex located at 72°N.

The subvolcanic Werner Bjerge alkaline complex (Bearth 1959) is one of the major intrusive centres in the lower Tertiary igneous province of East Greenland (Fig. 1). The complex is of interest because of the wide range of rock types represented, including kaersutite-bearing gabbroic rocks, alkali syenite, alkali granite and nepheline syenite. Further, extensive pneumatolytic and hydrothermal activity associated with the complex has given rise to mineralisation of considerable economic interest. This includes a major disseminated molybdenum deposit at Malmbjerg (Bearth 1959, Kirchner 1964) and a now exhausted galena and sphalerite vein-deposit at Mesters Vig (Bondam & Brown 1955).

Recent reviews of the Tertiary igneous activity in East Greenland include Brooks (1973), Noe-Nygaard (1974, 1976) and Deer (1976). The Werner Bjerge complex forms part of a zone of subvolcanic centres traceable for about 120 km, from Kap Parry towards south-west Scoresby Land across the late Palaeozoic to Mesozoic platform sediments bordering the East Greenland Caledonian mountain belt (Fig. 2). No plateau basalts are found in this area, but the subvolcanic centres cut a sequence of tholeiitic sills with compositions similar to the plateau basalts elsewhere in East Greenland (cf. Noe-Nygaard 1976). The Werner Bjerge complex is located at the continental, i.e. south-western, end of this zone of intrusions, although aeromagnetic evidence indicates an additional small pluton to the south-west which is not exposed (H. C. Larsen, pers. comm.). The complex is emplaced into flat-lying late Palaeozoic sediments immediately east of the main normal fault marking the western boundary of the post-Caledonian sedimentary basin.

Radiometric dating of syenites from the Werner Bjerge complex yields a whole rock Rb/Sr age of 30 ± 2 Ma (Rex et al. 1979) and fission track ages on sphenes give 30.3 ± 1.3 Ma (Gleadow & Brooks 1979). This is the youngest age so far reported from the Tertiary igneous province of East Greenland. No radiometric dating of the older gabbros has yet been carried out so that their precise relationship to the syenites is in doubt.

The occurrence of nepheline syenite in this zone of intrusions is restricted to the Werner Bjerge complex. The other subvolcanic centres (Noe-Nygaard 1941, Schaub 1942, Kapp 1960, Engell 1975) are dominantly composed of rocks of syenitic and/or granitic compositions. Amphibole-bearing gabbroic rocks are known both from the Werner Bjerge complex (Bearth 1959) and the Theresabjerg complex (Kapp 1960). A wide spectrum of dykes associated with the intrusions in Scoresby Land has been described by Bearth (1959) and Kapp (1960).

Among the other Tertiary intrusions in East Greenland the closest parallel to the Werner Bjerge complex is the Kangerdlugssuaq intrusion (Wager et al. 1976). This intrusion consists of nordmarkite grading continuously into nepheline syenite. No basic cumulates are exposed in the Kangerdlugssuaq intrusion although kaersutite-bearing gabbroic inclusions have been described from the late dyke swarm which in part cuts the intrusion (Brooks & Platt 1975).

The present microprobe study of the mineralogy of the Werner Bjerge complex is based largely on the collection used by Bearth in his original description of the complex (Bearth 1959), which is now housed at the Geological Museum, University of Copenhagen. Unfortunately, the supply of the samples chemically analysed by Bearth appears to have been exhausted in the process, and thus none of these were available for the present study. The study was limited to the least altered of those samples whose location was readily identifiable and does not cover all rock types present in the complex. The investigation further includes some related kaersutite-bearing mafic inclusions from camptonitic dykes cutting the nearby Theresabjerg complex. The mineral analyses were made with an energy-dispersive TPD-microprobe at the Research School of Earth Sciences, Australian National University, Canberra, using the procedure described by Reed & Ware (1975).

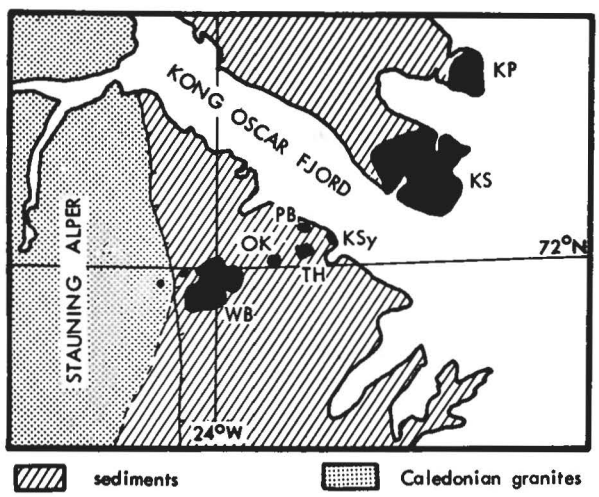

Fig. 2. Tertiary plutonic and sub-volcanic rocks around Kong Oscar Fjord, East Greenland. The area shown is located in Fig. 1. WB: Werner Bjerge; OK: Oksehorn; TH: Theresabjerg; PB: Pictet Bjerg; KSy: Kap Syenit; KS: Kap Simpson; KP: Kap Parry.

2. Geology

The geological map of the Werner Bjerge complex (Bearth 1959) is given in Fig. 3. The complex outcrops in a roughly circular area of mountainous terrain about 17 km in diameter. Exposures are confined to steep ridges between the glacier-filled valleys. The complex is subvolcanic in character with a partially preserved roof of feldspar porphyries, breccias and pyroclastic rocks. Among the intrusive rocks, three sub-complexes have

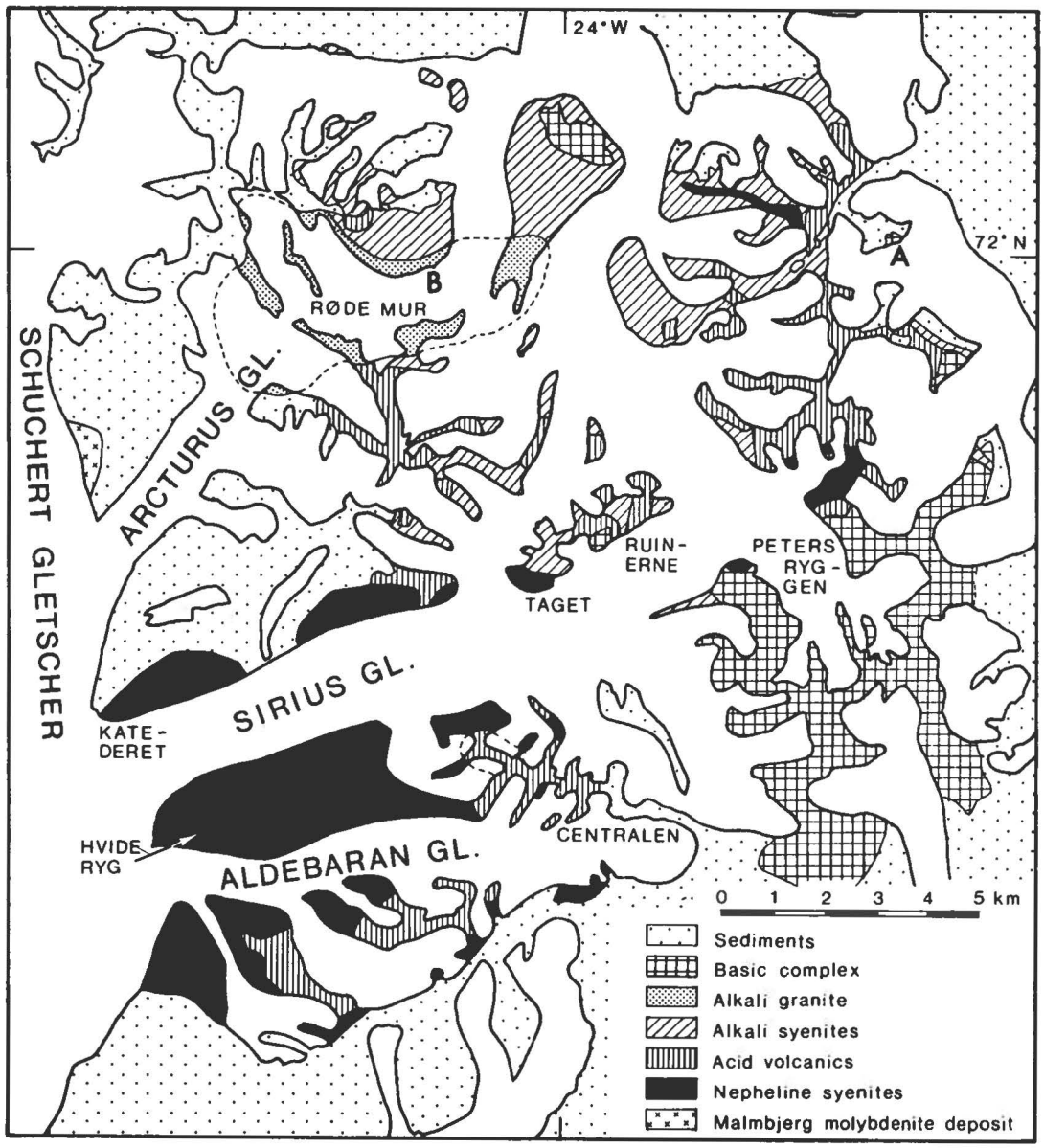

Fig. 3. The geology of the Werner Bjerge complex simplified after Bearth (1959). Localities A and B are referred to in Table 1.

been distinguished in terms of rock types (Bearth 1959): the basic complex preserved mainly in the south-eastern part of the area, the complex of alkali syenites and alkali granites dominating the northern sector and the nepheline syenite complex mostly occurring in the south-west.

The basic complex is the oldest of these sub-complexes. It is very heterogeneous with volcanic agglomerates and breccias, porphyritic marginal facies and coarse-grained internal facies showing both phase and cryptic layering as well as autobrecciation and veining by residual material. Rocks of the basic complex show a wide range of types: pyroxenites, kaersutite-bearing alkali gabbros grading into syenogabbros, syenites and granites were reported by Bearth (1959, p. 16). The syenogabbros and more leucocratic rock types invariably show autohydrothermal alteration of the primary minerals, thus the plagioclase in these rocks is more or less completely altered to saussurite. Among the dykes surrounding the Werner Bjerge complex, a suite of alkaline dykes of camptonitic affinity is thought to be related to the basic complex (Bearth 1959).

The northern sub-complex of alkali syenite and alkali granite is more complex than indicated on the map (Bearth 1959). These rocks typically show a banded alternation of grain size and texture and the development of pegmatoidal patches. Alkali granites and quartz porphyries are limited to a large body at the northern edge of the complex. The syenites pass imperceptibly through nordmarkites into nepheline-normative alkali syenites. The alkali syenites (generally quartz-normative) contain several minor bodies of sodalite-bearing pulaskites (Bearth 1959, p. 28). Unfortunately, the exact relationship between these rock types is unknown. In general, the pulaskites are richer in mafic minerals than the quartz-bearing syenites. In the latter rocks, the sparse mafic minerals are normally replaced by limonite but they are generally fresh in the pulaskites. The disseminated molybdenum deposit mentioned above is associated with this northern complex.

The nepheline syenite complex in the south-west consists of analcime-bearing alkali syenites grading into nepheline-sodalite foyaites. Again the rocks are characterised by a variable grain size and texture. Bearth (1959, p. 34) suggests that several generations of intrusions are involved and one of these is probably the youngest in the Werner Bjerge complex, except for the dykes. A group of tinguaitic dykes is closely associated with the nepheline syenite complex. In places the nepheline syenites contain xenoliths of the roof including feldspar porphyries and the arenaceous late Palaeozoic sediments. Pegmatites from the nepheline syenites contain areas with an interesting mineral paragenesis including narsarsukite, quartz, alkali feldspar, analcime, aegirine, calcite and occasionally fluorite (Bearth 1959, p. 33). Cracks filled with quartz and carbonates are also found in discontinuous zones of hydrothermally altered foyaite.

Major element analyses of the more important rock types from the Werner Bjerge complex are given by Bearth (1959). An alkali–silica diagram (Fig. 4) shows the chemical relationship of this complex to other sub-

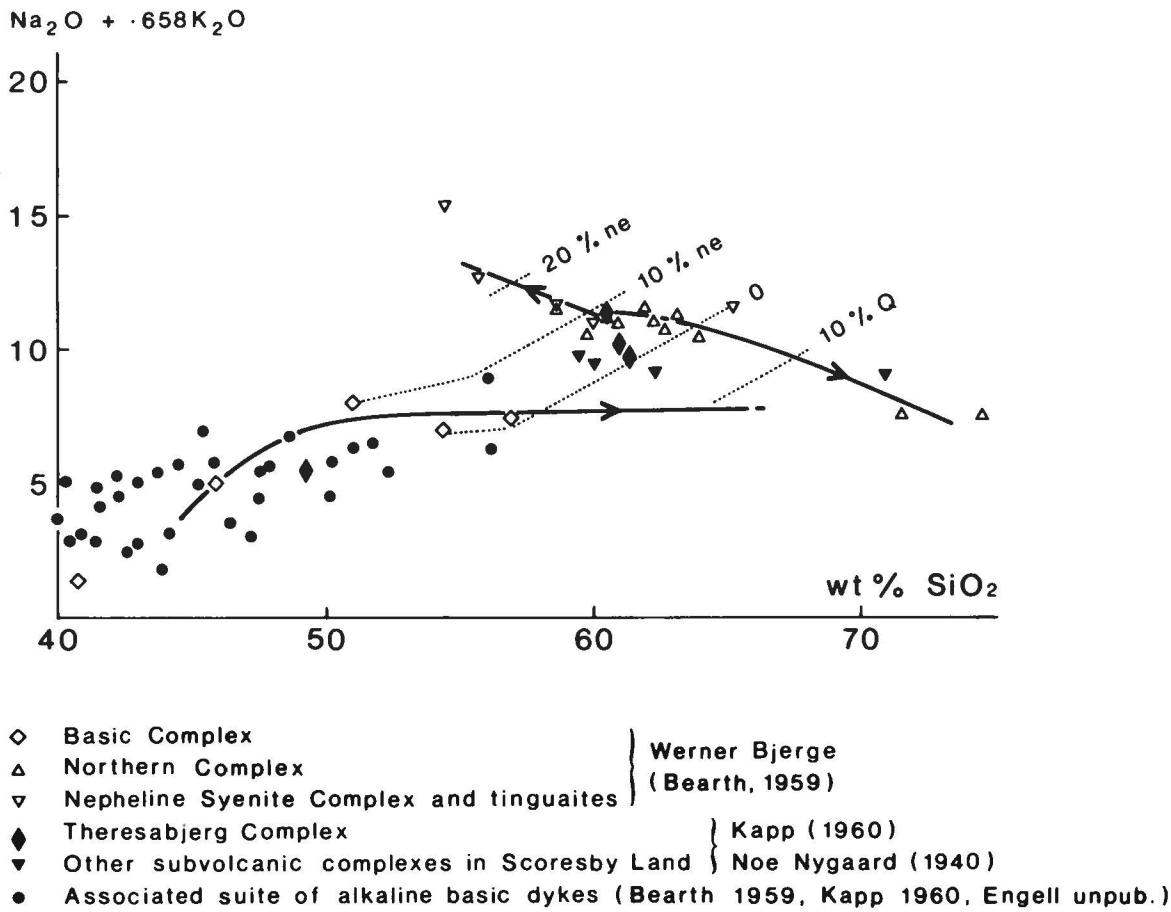

Fig. 4. Alkali–silica diagram summarising the relationships between various Tertiary rocks in the area of Werner Bjerge (Scoresby Land). All points are calculated on a water-free basis and alkalis are expressed in wt.% with K_2O recalculated to equivalent Na_2O. The dotted diagonal lines show approximate amounts of normative quartz or nepheline and the full lines show the general evolutionary trends of the Werner Bjerge rocks.

volcanic centres in the region (Noe-Nygaard 1941, Kapp 1960) and the associated suite of alkaline basic dykes (Bearth 1959, Kapp 1960, new unpubl. anal.) in Scoresby Land. It is possible that the felsic rocks of the Werner Bjerge complex and the other centres are derived from liquids similar to those represented by the alkaline basic dykes and we suggest that the degree of silica saturation at the syenitic stage may be controlled by the degree of amphibole fractionation. Further evidence for this is the amphibole-bearing syeno-gabbro stock in the Theresabjerg complex ("gabbro-diorit", Kapp 1960) and the kaersutite-bearing mafic inclusions (described here) from two camptonite dykes cutting this complex, which is of sub-volcanic character and consists of syenites, syenite-porphyries and the above-mentioned syeno-gabbro. The inclusions in these dykes are up to approx. 1/4 m in diameter and are reminiscent of those described by Brooks & Platt (1975) from the Kangerdlugssuaq district.

3. General petrography

The minerals previously known from the Werner Bjerge complex are listed by Bearth (1959, p. 62).

The specimens investigated here include five samples from the gabbroic part of the basic complex (one mafic cumulate and four gabbros), two granites from the northern complex, seven foyaites, one tinguaite dyke and one sample of a quartz- and narsarsukite-bearing pegmatite from the nepheline syenite complex. Further, as a supplement to the samples from the basic complex, three inclusions of kaersutite-bearing cumulates from two camptonitic dykes cutting the Theresabjerg complex have been investigated. Locations and brief notes on the investigated samples are given in Table 1. It should be noted that four of the five samples from the basic complex are from a minor stock, and thus closely related, whereas the last sample (WB 105) is from another part of the basic complex.

A summary of the mineralogy of the samples, including some of the more important information on mineral compositions, is given in Table 2. Below follow short petrographic descriptions of the major rock groups included in this investigation.

3.1 The basic complex

3.1.1 Mafic cumulates (WB 154). – This rock is a cumulate of the gabbroic minerals described below, i.e. clinopyroxene (approx. 70%), olivine, titanomagnetite

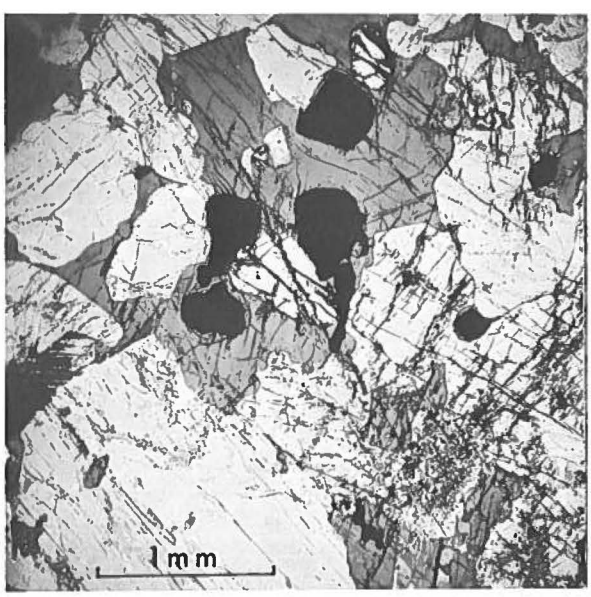

Fig. 5. Mafic cumulate, WB 154: with cumulus pyroxene (light grey), olivine (small crystals in kaersutite) and titanomagnetite with intercumulus kaersutite (dark grey).

Table 1. List of samples investigated in this study.

The Basic Complex	
WB 154	mafic cumulate, N side of glacier ("Escher von der Linth Gletscher") descending to SW head of Blomsterdal (marked "Antarctic Dal" on Bearth's map) where this outcrop of basic rocks is not marked. Locality A on Fig. 3.
WB 156	olivine gabbro, same locality.
WB 153	olivine gabbro, same locality.
WB 151	"diorite", same locality.
WB 105	syenogabbro, Petersryggen.
Mafic cumulates from Theresabjerg	
GGU 123714 GGU 123722 GGU 123736	inclusions in basic dykes
The Northern Complex	
WB 7	biotite granite, N side of Mellemgletscher (see map in Bearth, 1959, locality B on Fig. 3).
WB 8	alkali granite, same locality.
The Nepheline Syenite Complex	
GGU 114848	"foyaite", Centralen (collected by N. Henriksen).
WB 268	"foyaite", extreme point of Hvide Ryg between Aldebaran Gletscher and Sirius Gletscher.
WB 300	"foyaite", Katederet, N side of snout of Sirius Gletscher.
WB 258	"foyaite", inner part of Hvide Ryg.
WB 320	"foyaite", point of Hvide Ryg near WB 268.
WB 273	"foyaite", S side of upper part of Aldebaran Gletscher.
WB 82	"foyaite", Taget, N side Sirius Gletscher.
WB 253	pegmatite with narsarsukite, believed to come from Hvide Ryg but ambiguously localised in original note books.
WB 322	tinguaite, near WB 268 and WB 320.

Table 2. Summary of the mineralogy of the Werner Bjerge samples.

Rock type	gabbro	gabbro	gabbro	gabbro	gabbro	biotite granite	alkali granite	foyaite GGU	foyaite	foyaite	foyaite	foyaite	foyaite	foyaite	tingua-ite	pegma-tite
Sample no.	WB 154	WB 156	WB 153	WB 151	WB 105	WB 7	WB 8	114848	WB 268	WB 300	WB 258	WB 320	WB 273	WB 82	WB 322	WB 253
plagioclase (% An)	89–88	79–73	58–25	79–31	80–35	67–7	–	–	–	–	–	–	–	–	–	–
alkali feldspar (% Or)	–	–	+	–	+	46–93	perth.	homogen.	homogen.	perth.	(+)	+	perth.	perth.	+	+
nepheline	–	–	–	–	–	–	–	+	+	+	+(alt.)	+	+	+	+	–
cancrinite	–	–	–	–	–	–	–	+	+	–	?	–	+	–	+	–
analcime	–	–	–	–	–	–	–	–	–	+	(+)	–	–	–	+	–
sodalite	–	–	–	–	–	–	–	+	+	–	+(alt.)	+	+	(+)	+	–
olivine (% Fo)	76	72–71	60–59	57–52	65	–	–	–	–	–	–	–	–	–	–	–
pyroxene (% Ac)	di.	di-sal.	di-sal.	di-sal.	di-sal.	–	41–42	8–42	11–79	23–94	46–92	67–68	69–91	72–86	78–97	90–93
amphibole	several types, ++	kaers.(+)	–	–	–	–	Mn-richt.	–	–	hast-kat.	–	arfv.	–	kat.	–	Li-arfv.
biotite	+	+	++	+	+	+	–	–	++	(+)	(+)	(+)	++	+	–	taen.
chlorite, talc, etc.	+	+	+	–	–	+	–	–	–	–	–	–	–	–	–	–
garnet	–	–	–	–	–	–	–	mel.	–	and.	–	–	–	–	–	–
magnetite	+	+	+	+	+	+	+	?	+	+	+	+	+	?	+	–
ilmenite	+	+	+	+	+	+	–	?	+	–	+	?	+	?	–	–
pyrophanite	–	–	–	–	–	–	+	–	–	–	+	–	–	+	+	–
sphene	+	–	–	–	–	–	+	+	+	(+)	–	++	++	++	–	–
zircon	–	–	–	–	–	–	(+)	–	–	(+)	–	–	–	(+)	–	–
apatite	+	+	+	+	+	+	–	–	–	–	–	+	+	+	–	–
sulphides	–	pyrrh.	–	pyr.	pyr.	–	–	+	pyr. pyrrh. sph. gal.	pyr.	–	pyr. pyrrh.	+	pyr.	pyr. pyrrh. sph. (gal.)	–
others		chal.	cal.			quartz. pyro.	quartz. pyro. chev.		pyro. cal.	musc.	(aenig.) musc.			thomp. pyro.	kup.	quartz. nars. pect. cal.

several REE, Nb and Zr phases remain unidentified

Abbreviations

+	present in usual amounts	cal.	calcite	kaers.	kaersutite	pect.	Mn pectolite	taen.	taeniolite
++	present in unusually large amounts	chal.	chalcopyrite	kat.	katophorite	perth.	perthite	thomp.	thompsonite
(+)	present in small amounts	chev.	chevkinite	kup.	kupletskite	pyr.	pyrite		
–	absent					pyro.	pyrochlore		
		di.	diopside	mel.	melanite	pyrrh.	pyrrhotite		
aenig.	aenigmatite			musc.	muscovite				
alt.	altered	gal.	galena			richt.	richterite		
and.	andradite			nars.	narsarsukite				
arfv.	arfvedsonite	hast.	hastingsite			sal.	salite		
		homogen.	homogeneous			sph.	sphalerite		

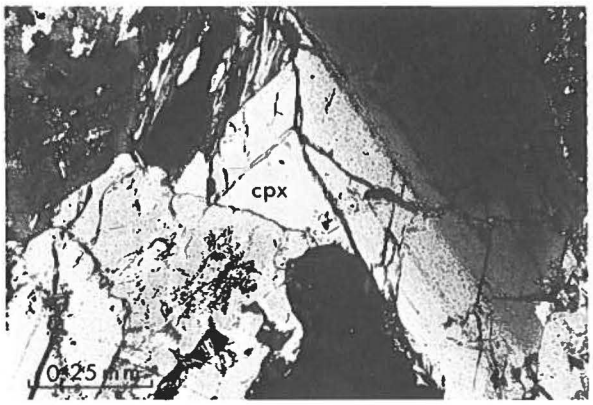

Fig. 6. Mafic cumulate, WB 154: showing continuous zoning from brown kaersutite (right) into late-stage colourless tremolite which coexists with colourless diopside (white triangular interstitial area, cpx), (× pol.).

and plagioclase (approx. 5%). Interstitially, kaersutite (approx. 10%) occurs instead of the brown mica in the gabbros (Fig. 5). The rock has two kinds of late-stage amphiboles, both very minor constituents; in a few cases continuous zoning from kaersutite into colourless tremolite coexisting with colourless diopside (also late-stage) is seen (Fig. 6), and in several cases the kaersutite is marginally replaced by green amphibole. Secondary sheet silicates (mainly replacing olivine) also occur.

3.1.2 Gabbros (WB 156, WB 153, WB 151, WB 105). – The main constituents of these rocks are plagioclase, clinopyroxene, olivine, Fe-Ti-oxide and mica, while minor constituents are apatite, kaersutite, alkali feldspar and secondary sheet silicates (Table 2). Plagioclase, olivine, clinopyroxene and titanomagnetite are euhedral cumulus phases (Fig. 7). The olivine occurs in subhedral corroded grains, and there seems to be no intercumulus olivine. The weakly zoned plagioclase laths are sharply rimmed by intercumulus, more Na-rich plagioclase, and interstitial K-feldspar may be present. The clinopyroxenes are light reddish-brown in thin section and have sub- to euhedral, nearly colourless cores (Fig. 8). The primary titanomagnetite crystals contain numerous exsolved ilmenite lamellae. Ilmenite also occurs as larger grains, but it is frequently intergrown with the titanomagnetite in a way suggestive of recrystallisation by granule exsolution, and it is doubtful whether there is any primary ilmenite. The Fe-Ti-oxide grains usually have fringes of deep red-brown pleochroic mica which also occurs as independent interstitial grains (Fig. 7). A few grains of interstitial kaersutite were found in one sample (WB 156). Sparse green biotite is presumably of post-magmatic origin, while the clearly secondary sheet silicates are granular or fibrous, light-coloured greenish, yellowish or brownish.

3.1.3 Mafic cumulates from dykes of the Theresabjerg complex (GGU 123714, 123722 and 123736). – These rocks contain almost the same phases as WB 154, but in varying amounts and with rather variable textures. Kaersutite is the dominant mineral in all three samples, and in 123714 it is interstitial as in WB 154, while in 123722 and 123736 it is euhedral and of cumulus as-

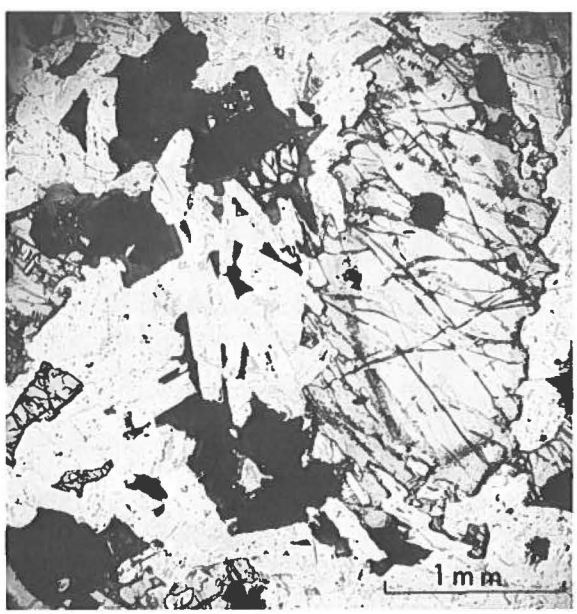

Fig. 7. Gabbro, WB 156: general texture with cumulus pyroxene (cored) and plagioclase with smaller cumulus olivine and titanomagnetite rimmed by late-stage mica.

Fig. 8. Gabbro, WB 151: showing light coloured diopsidic pyroxene core rimmed by later brown pyroxene, cumulus olivine and plagioclase (× pol.).

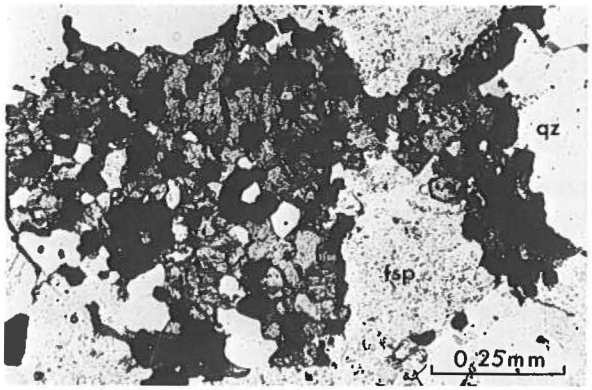

Fig. 9. Alkali granite, WB 8, with mafic aggregate consisting of magnetite, quartz, alkali pyroxene and alkali amphibole. Surrounding minerals are alkali feldspar (fsp) and quartz (qz).

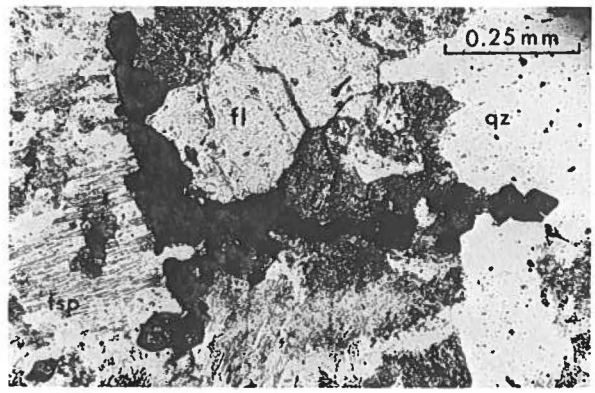

Fig. 10: Alkali granite, WB 8, showing a train of euhedral crystals of pyrochlore and chevkinite running approximately horizontally through the picture. Surrounding minerals are feldspar (fsp), quartz (qz), fluorite (fl, high relief) and alkali amphibole, which is speckled with small titanomagnetite grains (dark grey).

pect. Other cumulus phases are clinopyroxene, titanomagnetite and abundant apatite. Olivine is absent. One sample (123714) contains abundant pseudomorphs of a euhedral hexagonal prismatic mineral – a feldspathoid? – now replaced by fine-grained aggregates of muscovite and alkali feldspar. Minor late-stage and secondary phases are colourless diopside, green amphibole, green chlorite, sphene, calcite and epidote.

3.2 The northern complex

The two available samples from the northern complex are nordmarkitic rocks which have too little quartz to be granites and may be intermediate between the granites and the syenites at B in Fig. 3. They differ strongly from each other indicating the importance of further work on these rocks.

3.2.1 Biotite granite (WB 7). – This is a rather fine-grained granular rock with perthitic alkali feldspar, plagioclase (albite) and approx. 15% quartz. The mafic minerals often form aggregates; they are dark brownish to greenish biotite, magnetite with coarsely granule-exsolved ilmenite at the rims, and smaller discrete ilmenite crystals. It is uncertain whether any of the ilmenite is primary. Light green chlorite is secondary after biotite. Accessory phases are apatite and pyrochlore.

3.2.2 Alkali granite (WB 8). – This rock is slightly more coarse-grained than WB 7. Its main mineral is cryptoto microperthitic alkali feldspar. Quartz amounts to approx. 10%. The mafic minerals often form aggregates of silicates and oxides as in the biotite granite, but the silicates in the alkali granite are blue-green amphibole and green aegirine-augite. The aggregates consist of many small subhedral crystals of magnetite and quartz poikilitically enclosed in a mosaic af alkali pyroxene and alkali amphibole (Fig. 9). The texture suggests recrystallisation of an earlier mafic silicate. Pyrophanite occurs as patches and granules in the magnetite which is rimmed by sphene. Accessory phases are zircon, fluorite, pyrochlore and chevkinite (Fig. 10).

3.3 The nepheline syenite complex

3.3.1 Foyaites (GGU 114848, WB 268, WB 300, WB 258, WB 320, WB 273 and WB 82). – Within the general frame provided by the term 'foyaite', these rocks are quite variable and may, as done in the above listing, be arranged in a suite ranging from lesser to more differentiated types. Their main constituents are alkali feldspar, nepheline, sodalite, alkali pyroxene and alkali amphibole or biotite. Minor minerals are magnetite, sphene, cancrinite, fluorite and a number of phases occurring in only one or a few samples, see Table 2. The alkali feldspar crystals vary in shape from broadly equidimensional, in the least differentiated types, to flat tablets in the more differentiated types. Perthite exsolution ranges from barely to clearly visible and is occasionally very coarse. Nepheline and sodalite are usually euhedral, but sodalite also occurs interstitially. Cancrinite is interstitial. Dark green zoned alkali pyroxene is ubiquitous and texturally variable, ranging from euhedral to interstitial single crystals and aggregates. Aggregates with single-crystal outlines (Fig. 11) and widespread sponginess in the pyroxene due to numerous small inclusions testify to extensive recrystallisation of the more Ca-rich pyroxene. Salite is found in two samples as small corroded core remnants. Late-stage aegirine is usually inclusion-free. WB 258 contains sector-zoned aegirine (Fig. 12). Large euhedral sphene crystals are common in all samples. The seven foyaites fall into three groups according to the other mafic phases. a) WB 300, WB 258 and WB 320 contain primary titanomagnetite with incipient ex-

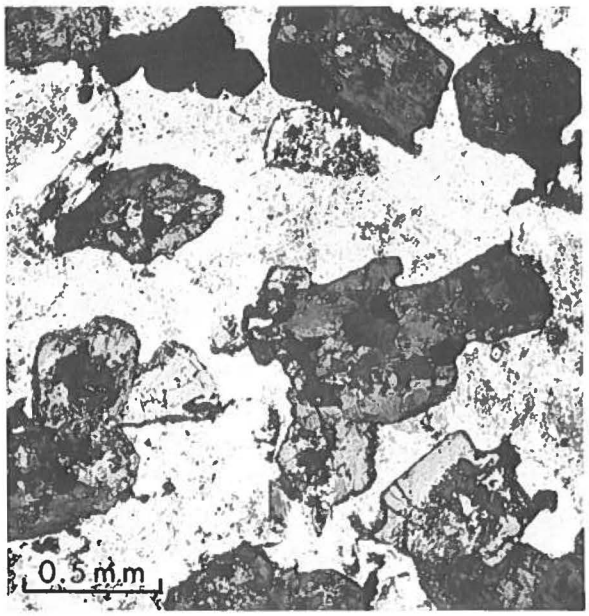

Fig. 11. Foyaite, WB 300: Euhedral crystals of pyroxene recrystallized to a mosaic of aegirine-augite with central amphibole patches.

solution features, alkali amphibole intergrown with and replacing the pyroxene (Fig. 11) and trace amounts of biotite. b) WB 268, WB 273 and WB 82 contain no amphibole or primary oxide. Instead, considerable amounts of biotite form intricate aggregates with the pyroxene and subordinate secondary magnetite and ilmenite-pyrophanite (Fig. 13). c) GGU 114848 contains almost solely alkali pyroxene, but one rather large area in the section consists of a fine-grained aggregate of pyroxene, sphene and brown melanite garnet.

3.3.2 Tinguaite (WB 322). – This is a green porphyritic dyke rock with 0.2–2 mm sized phenocrysts of

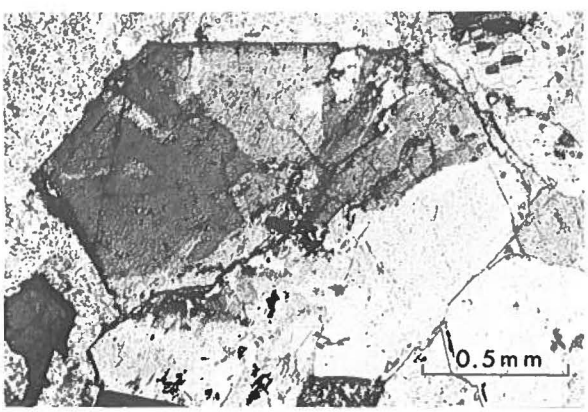

Fig. 12. Foyaite, WB 258: Sector-zoned aegirine crystal (× pol.).

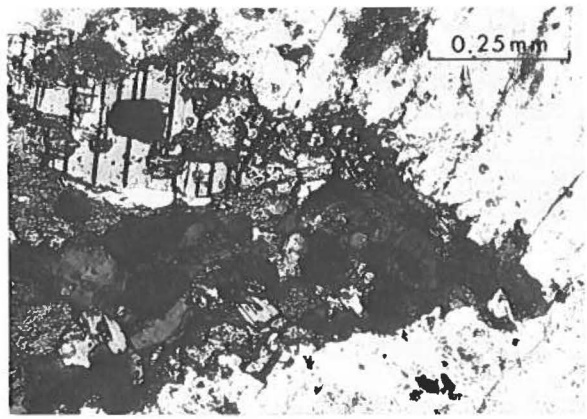

Fig. 13. Foyaite, WB 273: Alkali pyroxene-biotite-magnetite aggregate in alkali feldspar.

K-feldspar, nepheline, sodalite and completely recrystallised pyroxene in a very fine-grained matrix of acicular aegirine crystals embedded in the light minerals (Fig. 14). A number of accessories occur, as listed in Table 2. Some of these are unusual and demonstrate the agpaitic character of the rock.

3.3.3 Narsarsukite pegmatite (WB 253). – The detailed geology of this sample is not clear, but it is certain that the pegmatite, despite being quartz-bearing, belongs to the foyaite complex. In this respect it resembles the type locality at Narssârssuk where the pegmatite is also quartz-bearing but associated with feldspathoidal rocks (Ussing 1912, pp. 244–249). The sample is moderately

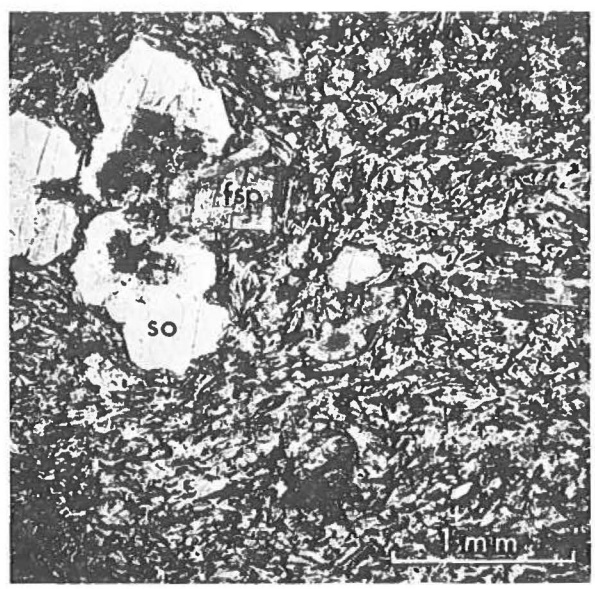

Fig. 14. Tinguaite, WB 322: phenocrysts of sodalite (so) and K-feldspar (fsp) in a felted groundmass of aegirine and light minerals.

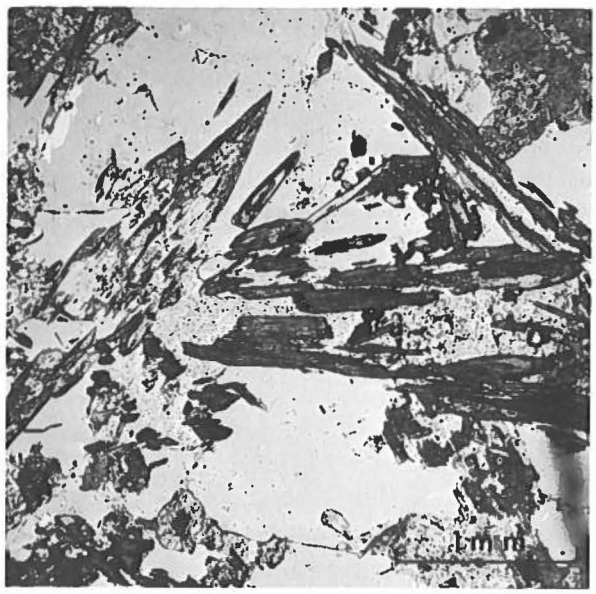

Fig. 15. Pegmatite, WB 253: showing aegirine needles and dusty K-feldspar in clear quartz.

coarse-grained and consists of approx. 50% quartz in which the other minerals are embedded. These are approx. 40% K-feldspar in box-shaped crystals showing chess-board twinning, and approx. 7% pale yellow-green aegirine in long acicular crystals and sheaf-like aggregates (Fig. 15). The remaining minerals are (in order of abundance): colourless, zoned narsarsukite in relatively few, large crystals (Fig. 16), small prisms of blue-green amphibole with colourless rims, small flakes of colourless mica (Figs 17 & 18), a few brownish grains of pectolite, and interstitial calcite.

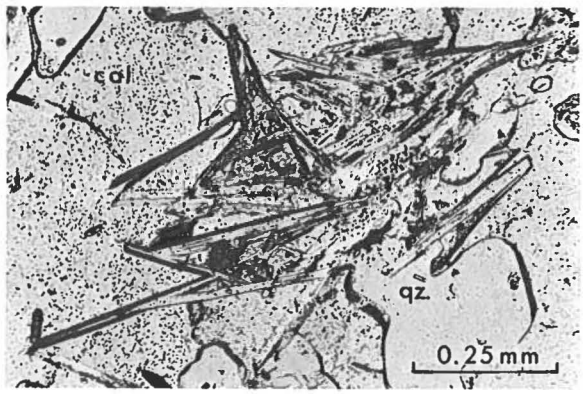

Fig. 17. Pegmatite, WB 253: with taeniolite needles and quartz (qz) in calcite (light grey, speckled, cal).

4. Mineralogy

4.1 Olivines

From Bearth's (1959) description it appears that the occurrence of olivine in the Werner Bjerge complex is restricted to the pyroxenites and gabbros of the basic complex. The present observations corroborate this; among the investigated samples, olivine was only observed in the five specimens from the basic complex. Further, no olivine pseudomorphs were observed in the other rock types, and they were also absent from the Theresabjerg inclusions.

Classified according to the olivine compositions (Table 2), the four samples from the small stock on the eastern flank of the complex form part of a differentiated sequence. Thus the olivines grade from Fo_{76} in virtually unzoned grains in the mafic cumulate (WB 154) through WB 156 and WB 153 to the most evolved gabbro (WB 151) with Fo_{57} in the core of large grains and Fo_{52} in small ones. The olivine in the gabbro from Petersryggen (WB 105) indicates that this sample rep-

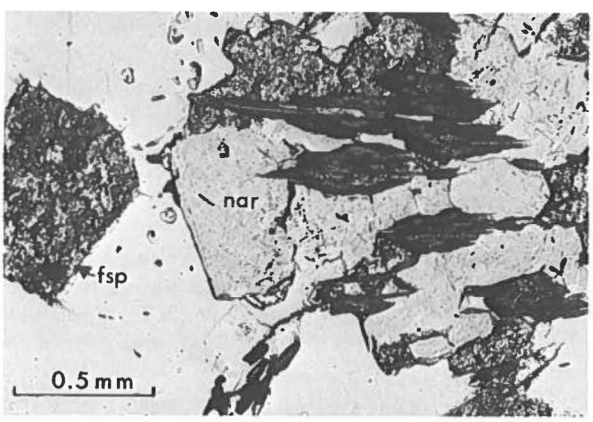

Fig. 16. Pegmatite, WB 253: with narsarsukite crystals (nar, grey, massive), aegirine (dark grey to black needles) and K-feldspar crystals (fsp) in clear quartz.

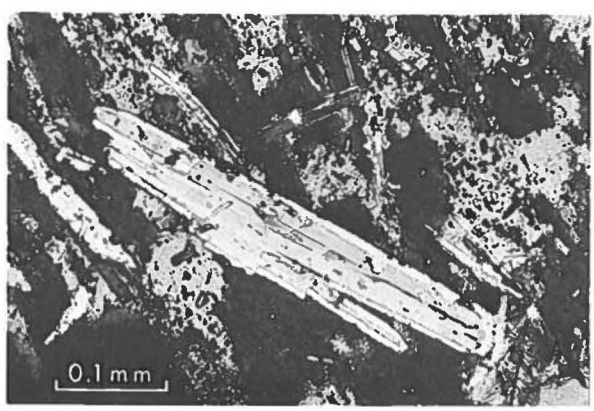

Fig. 18. Pegmatite, WB 253: taeniolite flakes in chess-board twinned K-feldspar (× pol.).

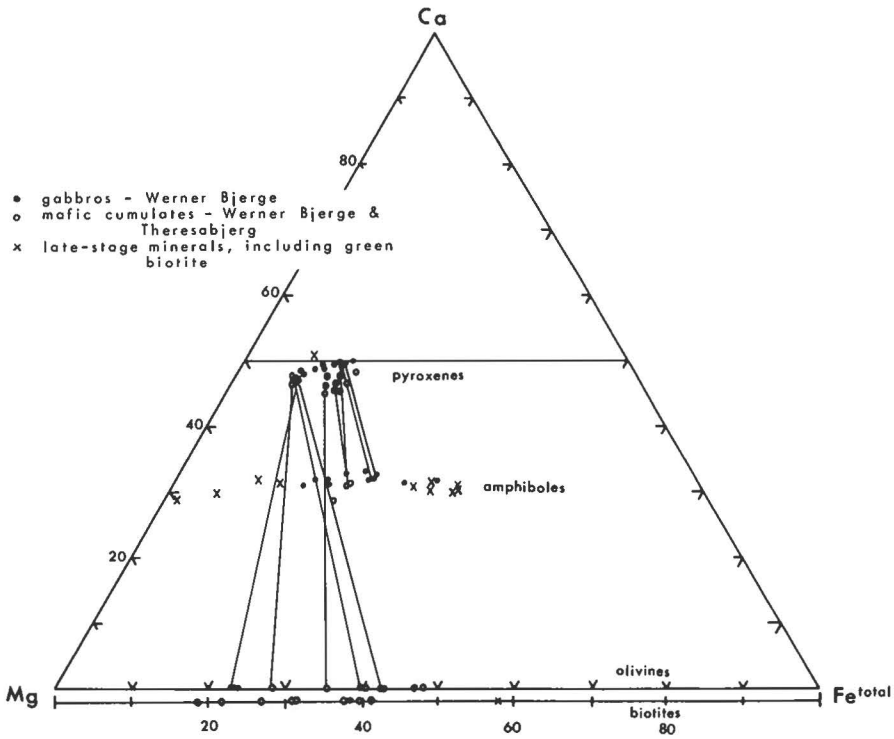

Fig. 19. Ca–Mg–Fe diagram for Werner Bjerge basic complex and Theresabjerg showing mutual relations among mafic silicates. Co-existing phases are joined by tie-lines.

resents an intermediate stage between WB 156 and WB 153 in a similar sequence.

The minor elements Ca and Mn in the olivines both increase with decreasing Fo content. CaO ranges from 0.0 to 0.6 %, while MnO ranges from 0.3 to 0.9 %. The contents of both elements are normal compared with the data of Simkin & Smith (1970) although the MnO contents in the more iron-rich of the Werner Bjerge olivines are slightly high.

4.2 Clinopyroxenes

4.2.1 Introduction. – Clinopyroxenes are present in all the investigated samples except for one of the granites from the northern complex (WB 7, Table 2). The spectrum of compositions covered by these pyroxenes, as well as the different fractionation trends observed, are illustrated by the familiar triangular diagrams in Fig. 19 and 20. The variation of selected elements is shown in Fig. 21, and analyses of representative pyroxenes are reported in Table 3. Fig. 19 also shows the variation relative to those of coexisting olivines, amphiboles and biotites.

4.2.2 The basic complex. – The pyroxenes of the one pyroxenitic and four gabbroic rocks investigated here are diopside-salite. Taken as a group, the pyroxenes show only a limited trend towards iron enrichment (Fig. 19), and the total variation in the hedenbergite component is 6.6–18.7 %. They are Ca-rich and Si-deficient, with slightly more Al than needed to fill the Z-position. The two most important silica-undersaturated components are $CaFe^{3+}AlSiO_6$ (0.3–8.8 %) and $CaTiAl_2O_6$ (0.6–7.4 %). The pyroxenes contain no wollastonite, but from 5.2 to 12.4 % orthopyroxene component. They are low in Na; the acmite component never rises above 4 % and there is no jadeite component (i.e. $Na<Fe^{3+}$, Al^{VI} calculated as $CaAl_2SiO_6$).

In contrast to the olivines, the core compositions of the pyroxenes are very similar and show no evolutionary trend. They are typical for pyroxenes crystallising from alkaline basic magmas (Carmichael et al. 1974, p. 273).

Some samples also contain a colourless, late-stage diopside which is believed to be formed by autohydrothermal processes. In strong contrast to the magmatic pyroxenes the post-magmatic ones are essentially silica-saturated and very poor in Ti and Al.

4.2.3 Kaersutite-bearing inclusions, Theresabjerg. – The pyroxenes from these inclusions are similar to those from the basic complex described above. They are slightly richer in acmite and the silica-undersaturated components.

4.2.4 Discussion of the diopside-salites. – Figs 19 to 21 show that, although the variations are small, each sample appears to have an individual fractionation trend.

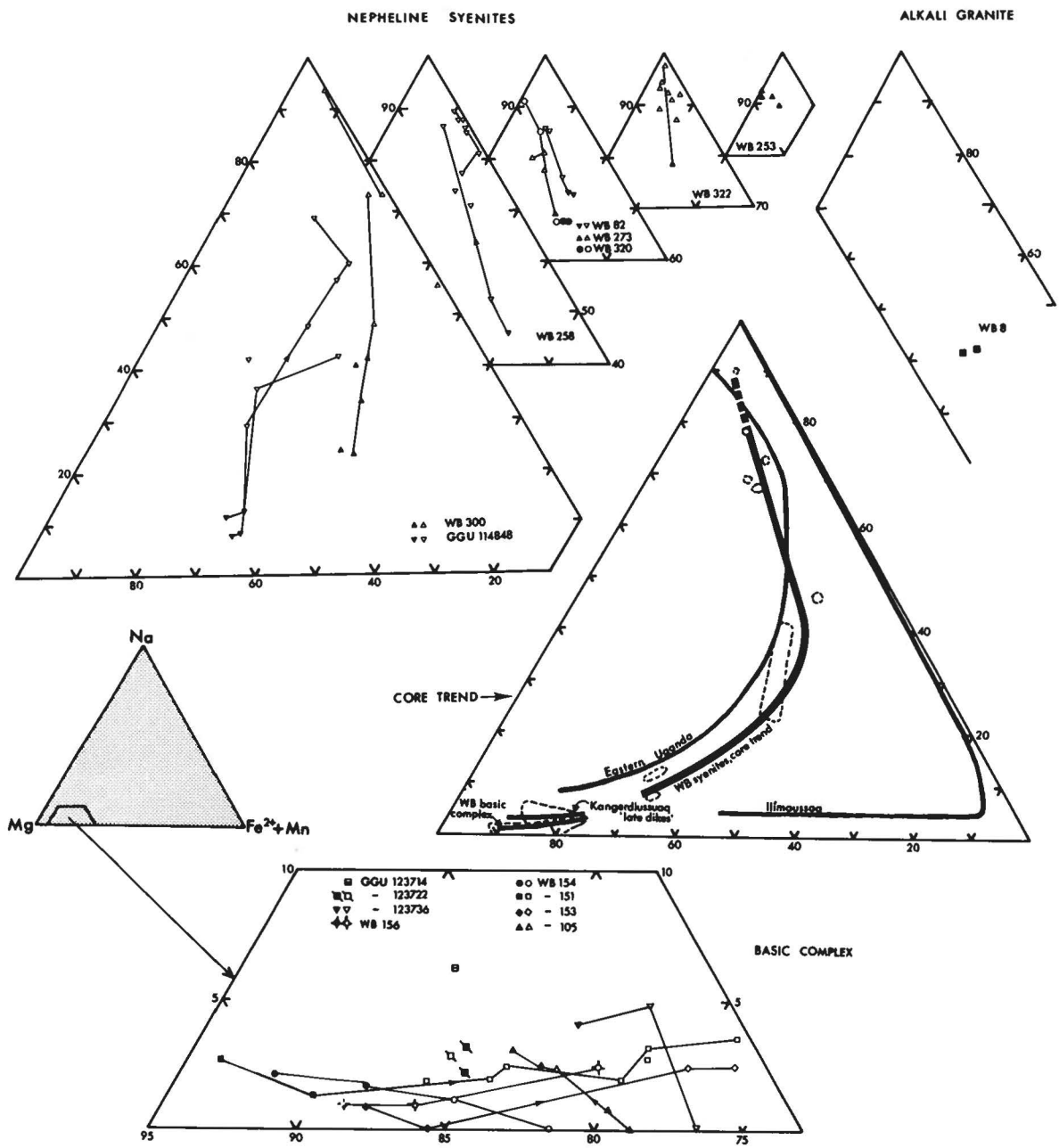

Fig. 20. Compositional variation in pyroxenes from the Werner Bjerge complex and Theresabjerg in terms of Mg–Na–(Fe^{2+} + Mn) – see key at left centre. The individual samples of foyaites together with the tinguaite (WB 322) and the narsarsukite pegmatite (WB 253) are shown at top left, the alkali granite at top right and the mafic rocks at the bottom. Centre right is a summary plot showing the overall trend of the pyroxene cores compared to trends of alkali pyroxenes from eastern Uganda (Tyler & King 1967) and Ilímaussaq (Larsen 1976). On this summary plot core fields of individual samples studied here are outlined by dotted lines. Closed symbols are cores, open symbols margins.

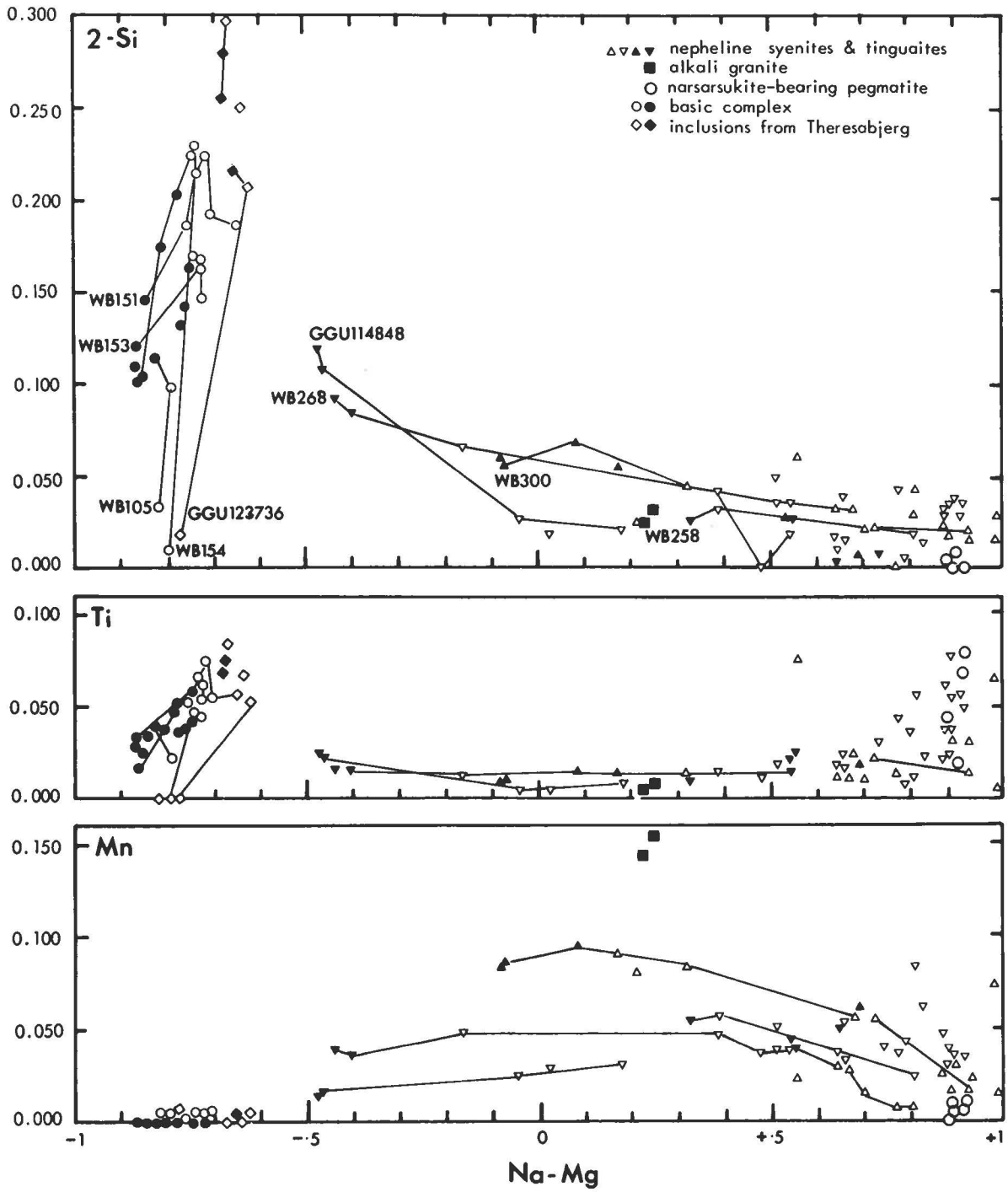

Fig. 21. Variation in compositions of pyroxenes in terms of the parameter Na–Mg (atoms per formula unit). Symbols are identified in the upper diagram. Closed symbols are cores, open symbols margins. Tie-lines indicate variation within individual crystals.

Table 3. Representative analyses of clinopyroxenes from Werner Bjerge.

	1	2	3	4	5	6	7	8	9	10
SiO_2	49.70	48.30	47.11	50.54	49.41	49.40	49.73	50.86	51.97	53.03
TiO_2	1.36	1.86	2.60	0.16	0.82	0.35	0.50	0.80	1.08	2.78
Al_2O_3	3.30	5.04	5.43	0.47	3.12	1.58	1.20	1.21	1.82	0.63
FeO	7.65	6.11	8.04	21.23	12.58	17.87	22.24	26.29	25.86	26.43
MnO	0.13	–	0.17	4.39	0.47	2.65	2.51	1.73	0.55	0.31
MgO	14.24	14.33	13.03	3.55	9.67	5.15	2.51	0.21	0.72	1.12
CaO	22.24	23.03	22.15	12.55	22.53	18.24	12.82	6.54	2.29	0.14
Na_2O	0.40	0.22	0.26	5.63	0.98	2.94	6.09	9.70	12.55	13.43
sum	99.02	98.89	98.79	98.54	99.58	98.18	97.60	97.34	96.84	97.91
Fe_2O_3	3.17	3.05	2.60	15.13	4.30	8.17	15.57	22.50	28.54	28.05
FeO	4.79	3.36	5.70	7.62	8.71	10.52	8.23	6.04	0.17	1.18
new sum	99.34	99.20	99.06	100.06	100.00	99.01	99.17	99.60	99.69	100.73
Cations on basis of 4 cations total and 6 oxygens										
Si	1.859	1.802	1.778	1.975	1.881	1.944	1.959	1.985	1.982	2.000
Ti	0.038	0.052	0.074	0.005	0.023	0.010	0.015	0.023	0.031	0.079
Al	0.146	0.222	0.242	0.022	0.140	0.073	0.056	0.056	0.082	0.028
Fe^{3+}	0.089	0.086	0.074	0.445	0.123	0.242	0.462	0.661	0.819	0.796
Fe^{2+}	0.150	0.105	0.180	0.249	0.277	0.346	0.271	0.197	0.005	0.037
Mn	0.004	–	0.006	0.145	0.015	0.088	0.084	0.057	0.018	0.010
Mg	0.794	0.797	0.733	0.207	0.549	0.302	0.148	0.012	0.041	0.063
Ca	0.891	0.921	0.896	0.526	0.919	0.769	0.541	0.274	0.094	0.006
Na	0.029	0.016	0.019	0.427	0.072	0.224	0.465	0.734	0.928	0.982
mg*	83.8	88.4	79.8	34.4	65.3	41.0	29.4	4.5	64.1	57.3

* mg = 100 Mg/Mg+Fe^{2+}+Mn

Key to Table 3

The basic complex

1. WB 105: core of light coloured pyroxene of cumulus aspect.
2. WB 154: light coloured diopsidic core.
3. WB 151: red-brown salite rim on light coloured core.

The northern complex

4. WB 8: aegirine augite of alkali granite.

The nepheline syenite complex

5. GGU 114848: light coloured salite core.
6. WB 300: light coloured aegirine augite core.
7. WB 300: inner part of green rim on previous, aegirine augite.
8. WB 300: centre of prismatic aegirine.
9. WB 322: aegirine phenocryst of tinguaite.
10. WB 253: titan-aegirine prism in quartz, coexisting with taeniolite, narsarsukite, etc.

There is no marked acmite enrichment, and there is a distinct gap between these pyroxenes and the most Na-poor salites from the salic rocks.

In Fig. 22, the Al-tschermakite and Fe^{3+}-tschermakite components in the pyroxenes are plotted against each other. The figure shows that all rocks except WB 156 fall in individual areas, and that the three cumulates from Theresabjerg and the one from Werner Bjerge (WB 154) are grouped together at high tschermakitic contents, different from the gabbros. This links the Theresabjerg rocks even closer to the Werner Bjerge rocks, and it is very probable that they were formed from magmas of essentially the same composition.

The Fe^{3+}-tschermakite component is present in rather large amounts (up to 10.4 mol % in the cumulates). According to Huckenholz et al. (1969), this component is stabilised by oxidising conditions which are consistent with the high water contents of the parent magmas suggested by the presence of amphibole- and mica-rich basic dykes associated with the basic complex (Bearth 1959), and also of the basic dykes from Theresabjerg which contain the investigated inclusions (J. Engell, unpubl. data). However, the presence of olivine indicates that the f_{O_2} was not excessive.

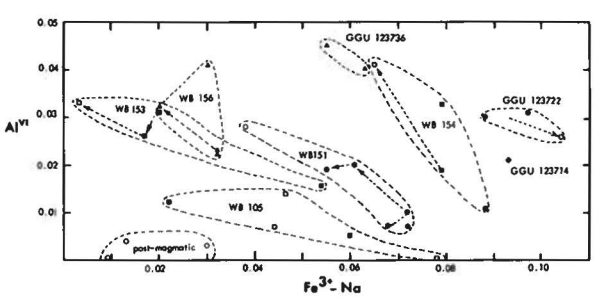

Fig. 22. Pyroxenes of the basic rocks plotted in terms of Al^{VI} and Fe^{3+}–Na, used to denote relative amounts of Tschermak's components. Closed symbols are cores, open symbols margins.

These pyroxenes are very similar to those described by Brooks & Platt (1975) from kaersutite-bearing gabbroic inclusions in late dykes cutting the Kangerdlugssuaq intrusion, which occur in an area of Archaean gneisses suggesting that the water-rich, oxidised nature of the camptonitic magmas at Werner Bjerge is not due to the sedimentary sequence in this area.

4.2.5 The northern complex. – Only one of the investigated granites contains pyroxene (WB 8). It is Mg-rich aegirine-augite with remarkably high MnO contents, ranging from 4.4 to 4.7 % (Fig. 21, Table 3). To the best of our knowledge, this is the highest MnO content ever reported for an igneous pyroxene. Manganoan aegirines are, however, known from metamorphosed manganese deposits (Deer et al. 1978).

The pyroxenes in WB 8 are slightly silica-deficient with less Al than needed to fill the Z-position, and a small excess of Fe^{3+} relative to Na.

4.2.6 The nepheline syenite complex. – The pyroxenes of the nepheline syenite complex span the interval from salite to aegirine (Bearth 1959). The investigated samples show individual pyroxene trends of essentially direct acmite enrichment (Fig. 20). However, variations in core compositions allow the seven investigated foyaites to be arranged into an evolutionary sequence (as in Fig. 20), to which the tinguaite dyke forms a natural continuation (Table 2 & 3).

The earliest pyroxenes in the least evolved foyaites (GGU 114848 and WB 268) are Ca-rich, Si-deficient salites (Table 3) with a strong affinity towards the pyroxenes from the basic complex although separated from them as noted above.

The trend defined by the pyroxene *cores* in the foyaites is characterised by an early enrichment in Na-pyroxene accompanied by a moderate change in the Fe^{2+}/Mg ratio (Fig. 20). It resembles the alkali pyroxene trends from the undersaturated alkaline complexes in Uganda (Tyler & King 1967) and Morotu (Yagi 1966), but differs strongly from the trend of the Ilímaussaq intrusion, which is also undersaturated and alkaline (Larsen 1976). The indication is that the pyroxenes in the foyaites began to crystallise under conditions where f_{O_2} was moderately high and not controlled by a FMQ type redox-reaction (Nash & Wilkinson 1970, Larsen 1976). The core trend does not necessarily imply that the foyaites represent samples of a single differentiating magma, but indicates some general, presumably environmental, control of f_{O_2} during the early stages of crystallisation of the involved melts. It is notable that the aegirine-augite from the granite (WB 8) and the aegirine from the narsarsukite pegmatite also lie on this core trend.

The individual, often irregular, trends of acmite enrichment observed within each of the different foyaite samples indicate that f_{O_2} was controlled by local conditions during the solidification of the intercumulus material (cf. Nash & Wilkinson 1970, Stephenson 1972).

Both the core trend and the individual pyroxene trends show depletion in the silica-undersaturated components with increasing Na contents (Fig. 21). The pyroxenes from the nepheline syenites are further characterised by low and fairly uniform Ti-contents except in the sodic varieties from the more evolved rocks (e.g. sector-zoned grain in WB 258 and the tinguaite WB 322) which show variable but generally higher Ti-values (Fig. 21). In the salites and the calcic aegirine-augites, Ti occurs dominantly as $CaTiAl_2O_6$, while in the more sodic pyroxenes this component is replaced by $NaTiAlSiO_6$ and Na $(Fe^{2+}, Mg)_{1/2}$ $Ti_{1/2}$ Si_2O_6, and high Ti values in the sodic pyroxenes reflect enrichment in the latter component (Table 3). In common with other sector-zoned aegirines (Larsen 1981), the sector-zoned grain in WB 258 shows particular enrichment of Ti in the (110) sectors and of Al in the (010) sectors.

The MnO contents in these pyroxenes are high, up to 2.9 %. Among alkaline undersaturated rocks these values are only rivalled by those in pyroxenes from the Kangerdlugssuaq intrusion (Kempe & Deer 1970, Brooks & Gill in press). The core trend is characterised by a strong increase in MnO (from 0.5 to 2.8 %) while the individual pyroxene trends maintain the different degrees of Mn-enrichment at fairly constant levels except for a decline in the more sodic pyroxenes (Fig. 21). Some of the scatter at the sodic end of the Mn-diagram in Fig. 21 is, like that for Ti, caused by the sector-zoned aegirine grain in WB 258 which is enriched in MnO, particularly in the (001) sector.

In contrast to the basic complex, the salites from the nepheline syenite complex contain essentially no excess of the orthopyroxene component (max. 0.9 %). This presumably reflects a difference in silica activity in the corresponding magmas. The more sodic pyroxenes from the foyaites and the tinguaite tend to have a small excess of wollastonite ($Ca_2Si_2O_6$ = 1 % to max. 4.6 %) whereas the aegirine-augite in the granite WB 8 and the aegirine from the quartz-bearing narsarsukite pegmatite contain a small excess of the orthopyroxene component (about 5 % and 1 % respectively).

The weakly zoned titan-aegirines from the narsarsukite pegmatite (WB 253) are essentially silica-saturated and poor in CaO, MnO and Fe^{2+}, but have comparatively high MgO and TiO_2 contents (Fig. 20 & 21, Table 3). The most important components are thus acmite (79.4–87.8%) and $Na(Mg, Fe^{2+}, Mn)_{1/2}$ $Ti_{1/2}$ Si_2O_6 (6.8–16.0%). The content of the Ti-components decreases as the acmite content increases. Similar late-stage pyroxenes are known from several other alkaline complexes, both oversaturated and undersaturated (cf. Rønsbo et al. 1977, Ferguson 1977, Nielsen 1979).

4.3 Amphiboles

4.3.1 Introduction. – In addition to clinopyroxene, many of the investigated samples contain amphiboles (Table 2). They range from kaersutites in the basic complex and the Theresabjerg inclusions, through hastingsites and katophorites to arfvedsonites in the nepheline syenites, and richterites in the oversaturated complex. The narsarsukite pegmatite was found to contain unique lithian and lithian titanian magnesio-arfvedsonites. The extreme range from calcic to sodic amphibole compositions covered by these rocks is illustrated in Figs 23 and 24, and representative analyses are given in Table 4.

The analytical data have been rationalised according to the general formula $AX_2Y_5{}^{VI}Z_8{}^{IV}O_{22}$ $(OH, F, Cl)_2$ assuming that vacancies occur only in the A-position, and (except for the lithian amphiboles) Fe^{3+} has been calculated by normalising total cations excluding (Ca+Na+K) to 13 and adjusting the charge balance to 46. By this procedure orthorhombic (Mg, Fe) amphibole components are left out of consideration. The classification scheme of Leake (1978) has been followed.

4.3.2 The basic complex. – According to Bearth (1959, table 1) amphiboles are present throughout the basic complex. However, only two of the five rocks studied here contain amphibole, namely the pyroxenitic cumulate and the most primitive gabbro (WB 154 and 156, Table 2). The main primary amphibole is brown kaersutite. Late-stage amphiboles in WB 154 are colourless magnesio-hornblende zoned to tremolite and green magnesian hastingsite/ferroan pargasite zoned towards actinolite. These are subordinate in amount.

4.3.3 Kaersutite-bearing inclusions, Theresabjerg. – The three mafic inclusions all contain kaersutite, and one of them (123736) contains sparse late-stage green magnesian hastingsite sharply rimmed by almost pure actinolite.

4.3.4 Discussion of the kaersutites and late-stage amphiboles. – The kaersutites contain from 4.5% to 6.5% TiO_2. With one exception they contain slightly more Al than needed to fill the Z-position. A possible primary evolutionary trend for the two Werner Bjerge samples is defined by an increase in the fractionation parameter Na+K–Ca (–1.17 to –1.07 in WB 154; –0.94 to –0.73 in WB 156) paralleled by a general increase in Si and Ti (Fig. 24) and a decrease in Al both in the Z and Y positions. There is, however, no correlation between this trend and the variation in total iron, estimated Fe^{3+}, or the number of vacancies (0.044–0.226 per formula unit). The amphiboles show a general trend of increasing Fe which parallels that of the coexisting pyroxenes (Fig. 19).

The kaersutites from Theresabjerg include more

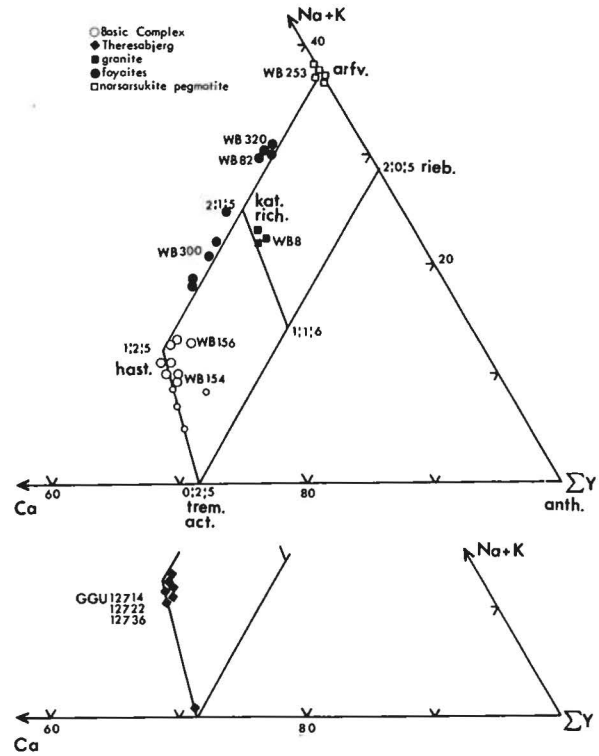

Fig. 23. The Werner Bjerge and Theresabjerg amphiboles showing relative amounts of octahedral and higher coordinated cations. For clarity, not all analyses have been plotted. The slightly smaller circles for the basic complex represent late-stage amphiboles. Abbreviations are: trem. = tremolite, act. = actinolite, anth. = anthophyllite, hast. = hastingsite, kat. = katophorite, rich. = richterite, arf. = arfvedsonite, rieb. = riebeckite.

Si-deficient types. They have generally higher Fe^{2+}+Mn/Mg+Fe^{2+}+Mn ratios than the Werner Bjerge kaersutites (0.32–0.49 against 0.26–0.33) and higher K/K+Na ratios (around 0.35 against generally less than 0.2).

In terms of Ca and Na the distinction is not so much between kaersutites from Werner Bjerge and Theresabjerg, but between kaersutites from the mafic cumulates and the gabbro. As shown in Fig. 25, the gabbroic kaersutites tend to be low in Ca and are high in Na+K, and this gives rise to a katophorite component in these.

The late-stage colourless and green amphiboles show a zonation towards pure Ca_2 $(Mg, Fe)_5$ Si_8O_{22} $(OH)_2$. They have progressively increasing Si contents, and decreasing Al and Ti. (Fig. 24). The number of vacancies increases while the alkalies and the K/K+Na ratio decrease. The difference between the two kinds of amphibole lies in the Fe/Mg ratios: the colourless amphiboles have higher Mg-contents than the kaersutites, the trend ending with nearly pure tremolite (Table 4, no. 1), while the green amphiboles have higher iron contents than the kaersutite they replace, approaching actinolite. This latter trend is not as extreme as that towards tremolite. In two cases in WB 154, a high con-

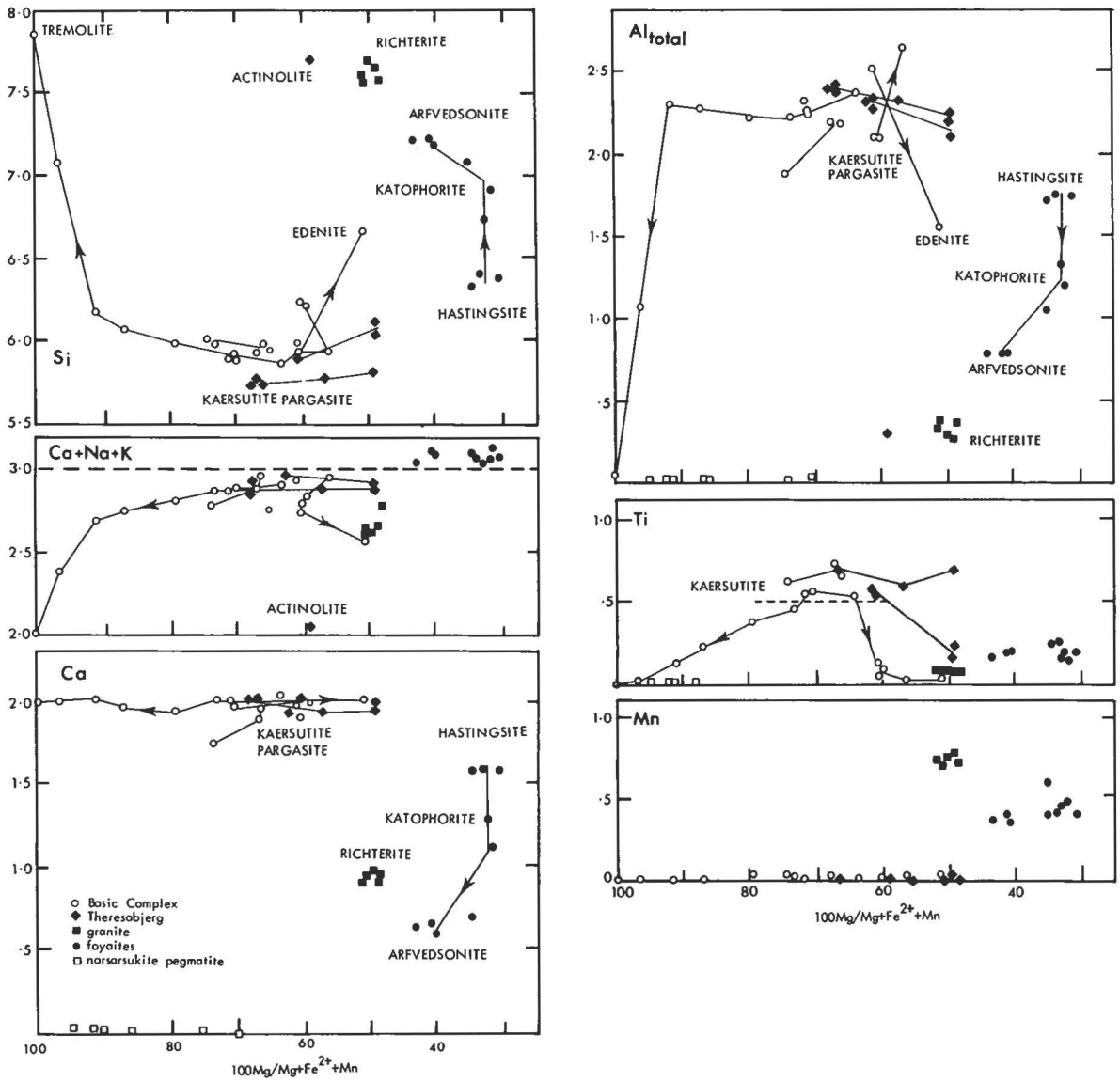

Fig. 24. Compositional variation in amphiboles as a function of Mg/Mg + Fe^{2+} + Mn for a number of cations. Zoning in single crystals is indicated by tie-lines. The broken line in the Ca + Na + K diagram denotes the maximum occupancy in A + X. That in the Ti diagram indicates the conventional lower limit for kaersutite.

tent of tschermakite (up to 31%), without actinolite, was encountered. These very different trends in the late amphiboles indicate the absence of an overall control of equilibrium in the late- to post-magmatic stages.

The MnO content is uniformly low in all the above described amphiboles, being slightly lower in the Werner Bjerge amphiboles than in those from Theresabjerg (0–0.23% against 0.17–0.33%). Two green late-stage amphiboles from Theresabjerg (123736) contain 1.35%–1.45% Cl whereas all the other amphiboles contain less than 0.07% Cl.

The primary kaersutites described here are very similar to those described by Brooks & Platt (1975) from inclusions of kaersutite gabbro in the late dyke swarm of Kangerdlugssuaq. Similar amphiboles are well known from basic units associated with other alkaline complexes, e.g. Shefford Mountain, Quebec (Frisch 1970).

Table 4. Representative analyses of amphiboles from Werner Bjerge.

	1	2	3	4	5	6	7	8	9	10	11
SiO_2	57.78	43.49	39.52	41.59	44.33	50.06	40.28	42.80	46.70	56.87	56.64
TiO_2	–	1.17	4.94	0.64	0.19	0.52	1.91	1.52	1.69	0.33	4.96
Al_2O_3	0.38	13.73	13.23	11.92	8.74	1.56	9.26	7.13	4.35	0.34	0.45
FeO	1.55	6.26	9.83	17.17	20.19	16.94	21.97	22.42	22.02	14.59	10.59
MnO	–	–	–	–	0.15	5.76	2.74	3.23	2.61	0.49	0.20
MgO	24.15	17.28	13.62	11.08	9.76	9.21	6.29	5.98	7.19	11.18	10.10
CaO	13.68	13.25	12.55	12.49	12.47	5.68	9.45	7.69	3.61	0.09	0.17
K_2O	–	0.26	1.10	0.85	0.26	1.19	1.54	1.61	1.85	1.86	1.75
Na_2O	–	2.28	2.31	2.37	1.75	4.94	3.91	4.79	7.18	9.71	9.34
($Li_2O_{calc.}$)	–	–	–	–	–	–	–	–	–	(2.78)	(3.51)
Sum	97.54	97.92	97.09	98.11	97.84	95.86	97.35	97.17	97.19	98.17	97.70
basis				Z + Y = 13				total cations = 16		Si = 8.000	
Si	7.864	6.176	5.882	6.214	6.676	7.651	6.296	6.693	7.189	8.000	8.000
Ti	–	0.125	0.553	0.072	0.022	0.060	0.225	0.178	0.196	0.035	0.527
Al	0.061	2.299	2.321	2.100	1.552	0.281	1.706	1.313	0.790	0.056	0.075
Fe^{3+}	0.075	0.393	–	0.486	0.464	0.742	0.744	0.720	0.744	1.644	0.943
Fe^{2+}	0.101	0.351	1.223	1.660	2.079	1.423	2.127	2.211	2.092	0.074	0.308
Mn	–	–	–	–	0.019	0.746	0.363	0.428	0.340	0.057	0.024
Mg	4.899	3.657	3.021	2.467	2.191	2.098	1.466	1.394	1.650	2.346	2.126
Ca	1.995	2.016	2.031	2.080	2.012	0.930	1.583	1.288	0.595	0.014	0.026
K	–	0.047	0.209	0.162	0.050	0.232	0.306	0.322	0.363	0.334	0.315
Na	–	0.628	0.667	0.687	0.511	1.464	1.185	1.454	2.143	2.651	2.558
($Li_{calc.}$)	–	–	–	–	–	–	–	–	–	(0.788)	(0.997)
mg*	100.0	91.2	71.2	59.8	51.1	49.2	37.0	34.6	40.4	94.7	86.5

* mg = 100 Mg/Mg + Fe^{2+}+Mn. Fe^{3+} was calculated by assuming 46 negative charges in the formula unit.

Key to Table 4

The basic complex

1. WB 154: tremolite – late stage colourless amphibole occurring as a sharply defined epitaxic rim on kaersutite.
2. WB 154: pargasite – outer part of zoned rim on kaersutite with a slightly smoky colour.
3. WB 154: kaersutite – large brown, primary amphibole.
4. WB 154: magnesian hastingsite – green amphibole, apparently replacing brown.
5. WB 154: ferro-edenitic hornblende – green area in kaersutite with apparently continuous zonation from kaersutite.

The northern complex

6. WB 8: manganoan richterite.

The nepheline syenite complex

7. WB 300: potassic manganoan magnesian hastingsitic hornblende – core of zoned crystal.
8. WB 300: potassic manganoan katophorite rimming pyroxene.
9. WB 320: potassic manganoan calcic arfvedsonite – large grain.
10. WB 253: potassian lithian magnesio-arfvedsonite – fine needles in quartz. Analysis corresponds to: $Rich_{1.5}$Li–Ti $Arfv_{3.5}$ Li $Arfv_{71.8}Arfv_{2.9}$.
11. WB 253: potassian lithian titanian magnesio-arfvedsonite – centre of fine needles of previous. Analysis corresponds to: $Rich_{2.6}$Li–Ti $Arfv_{49.9}Arfv_{37.5}$Ti $Rieb_{2.5}Rieb_{7.3}$.

NB: In analyses 10 and 11 Li_2O is estimated as described in the text.

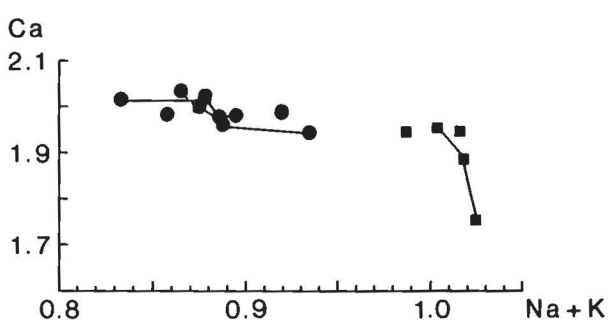

Fig. 25. Relationship between Ca and (Na + K) for kaersutites from Werner Bjerge and Theresabjerg. Mafic cumulates shown with closed circles; gabbros by solid squares.

4.3.5 The northern complex – Amphibole is not a common mineral in the oversaturated rocks. Riebeckite, arfvedsonite and rare 'barkevikite' (presumably manganoan hastingsitic hornblende) have earlier been reported from the pulaskites in this complex (Bearth 1959, p. 28).

In the alkali granite WB 8, the amphibole is manganoan richterite containing 5.42%–5.80% MnO (Table 4, Figs 23 and 24). This is the most manganese-rich amphibole encountered in this investigation, and it coexists with manganoan aegirine-augite. The amphibole is virtually unzoned, low in Ti and Al, and has slightly less Al than required to fill the Z-position to which accordingly some Fe^{3+} must be referred.

The relatively large number of vacancies (0.25–0.37 per formula unit) is well correlated with twice as much Fe^{3+VI} and represents a riebeckite component which consequently constitutes 25–37% of the mineral.

Richterites of similar compositions but with lower MnO contents are well known from moderately alkaline oversaturated rocks, e.g. alkali granite from Skye (Thompson 1976) and quartz trachytes in the Trans-Pecos province (Barker & Hodges 1977). An arfvedsonite with as much as 10.83% MnO was recorded from an alkali granite from the Oslo province by Neumann (1976), and other amphiboles from alkali granites in this province also show high MnO contents. Similar amphiboles from the nordmarkites of the Kangerdlugssuaq intrusion are reported by Kempe & Deer (1970) and Brooks & Gill (in press).

4.3.6 The nepheline syenite complex. – According to Bearth (1959, p. 30), the amphiboles from this complex include 'barkevikite' and arfvedsonite. Of the investigated samples only three of the foyaites and the narsarsukite pegmatite contain amphiboles (Table 2). The compositional variations of the amphiboles parallel the general evolutionary trend of the pyroxenes described above.

The amphiboles in the more primitive of the amphibole-bearing foyaites (WB 300) vary from manganoan magnesian hastingsitic hornblende (Bearth's barkevikite?) to manganoan katophorite whereas the two evolved foyaites (WB 258 and 320) contain calcian manganoan arfvedsonite (Table 4, Figs 23 and 24).

Thus, as in other alkaline undersaturated complexes (cf. Frisch 1970, Larsen 1976) the principal substitution is one of NaSi for $CaAl^{IV}$ in response to the increasing peralkalinity of the melts as monitored by the acmite content of the pyroxenes.

There is a clear relation between the composition of amphibole and pyroxene in any rock. Thus WB 300 contains the most Ca-rich and most zoned pyroxenes and amphiboles, whereas WB 320 contains the most acmite-rich pyroxene and the most sodic amphibole (arfvedsonite). Similar relationships were observed in several other alkaline rocks (Stephenson 1972, Larsen 1976, Ferguson 1977).

In all amphiboles from the foyaites the sum of Ca, Na and K is greater than 3.00 when the analyses are rationalised as described above (Table 4). This indicates either the break-down of the calculation scheme or the occurrence of an undetected element in the Y-position. Therefore the estimated Fe^{3+} content cannot be considered accurate. However, the general tendency of increasing Fe^{3+} and constant or slightly decreasing values of $Fe^{2+}+Mn/Mg+Fe^{2+}+Mn$ are considered reliable.

The amphiboles from the foyaites are further characterised by a low Al^{VI} content, a moderate and fairly uniform Ti content and a high and somewhat variable Mn-content (MnO 2.61–4.30%). Although uncommon in undersaturated alkaline complexes, the high MnO content is not exceptional. Frisch (1970) thus reported values of 3.20–4.30% MnO in hastingsite-katophorites from Shefford Mountain, Quebec, and an arfvedsonite with over 3% MnO has been reported from the Kangerdlugssuaq intrusion (Kempe & Deer 1970).

The amphibole in the narsarsukite pegmatite is light-coloured to bluish magnesio-arfvedsonite, but the sums of the microprobe analyses are low and charge balance cannot be achieved by the usual calculation procedure. The Si content of these amphiboles is high whereas Al is very low. If the probe-analysed cations are normalised assuming 8.000 Si per formula unit the sum of Ca, Na and K becomes very close to 3 (2.899–3.094; mean 3.006, st. dev. 0.054) whereas the sum of the remaining cations assigned to the Y-position is low (4.003–4.351). Semi-quantitative analyses made by laser-excited optical emission spectrography indicate that these amphiboles contain appreciable amounts of Li_2O (1.5%).

Considerations based on ionic radii make it reasonable to assume that Li can substitute for Mg in the Y-position in amphiboles and it is assumed that the deficiency in the Y-position in the recalculated probe analyses is due to the occurrence of Li. The amount of calculated Li is 0.649–0.997 cations per formula unit, equivalent to 2.28–3.51% Li_2O. The analyses have been rationalised on this basis and charge balance was obtained in 7 out of 8 cases with nearly all iron as Fe^{3+} (Table 4, Fig. 23). The blue amphiboles are lithian titanian magnesio-arfvedsonites containing up to 50% of an arfvedsonite component in which 3 Mg have been replaced by Li_2Ti. The light-coloured amphiboles, which rim the blue ones, are lithian magnesio-arfvedsonites containing up to 76% of an arfvedsonite component in which 2 Mg have been replaced by $LiFe^{3+}$.

These amphiboles appear to be unique, although eckermannite containing 1.15% Li_2O is known from nepheline syenite in Norra Kärr (Sundius 1945, analysis quoted by Deer et al., 1963), and Borley (1963) found 0.42–2.20% Li_2O in arfvedsonite from the Younger Granites of Nigeria. Lithian amphiboles are probably more widespread than suggested by the more recent literature, due to the inability of the microprobe to determine Li.

4.4 Sheet silicates

4.4.1 Introduction. – Nearly all the investigated samples contain one or more types of sheet silicate (Tabe 2). Micas of the phlogopite-biotite series are by far the most abundant while the narsarsukite pegmatite contains the rare Li-mica taeniolite and some of the nepheline syenites contain traces of muscovite. In addition, sheet silicates have also been formed at the expense of primary silicate phases by post-magmatic alteration processes and these are mixed-layer biotite-chlorite, chlorite and talc in the basic rocks and

Table 5. Representative analyses of sheet silicates from Werner Bjerge.

	1	2	3	4	5	6	7	8	9	10	11	12	13	14	15
SiO_2	33.07	36.05	35.19	36.19	35.70	37.65	36.06	43.44	59.19	39.87	34.54	34.09	24.40	23.13	48.97
TiO_2	0.43	7.80	8.56	7.49	2.95	3.40	3.00	–	–	–	–	–	0.13	0.13	0.10
Al_2O_3	17.58	14.96	14.40	13.59	11.41	10.71	10.68	38.87	–	2.14	9.58	11.73	15.99	19.71	0.17
FeO	15.22	11.87	14.08	14.51	29.25	21.30	24.58	1.01	–	10.07	13.89	25.16	33.60	39.17	6.59
MnO	–	–	–	–	1.21	2.04	4.06	–	–	0.17	–	0.14	0.67	1.79	–
MgO	20.12	15.04	12.84	13.46	5.65	10.55	6.77	–	19.22	33.94	27.55	15.35	7.81	4.21	32.85
CaO	0.31	0.28	0.17	–	–	0.17	0.09	–	–	0.27	0.20	0.66	0.15	–	0.46
K_2O	4.15	9.36	9.67	9.59	9.14	9.87	9.57	11.30	11.56	–	–	0.23	0.17	–	–
Na_2O	0.17	0.54	0.28	0.31	0.34	0.46	0.46	–	–	–	–	–	0.28	0.22	–
SO_3	–	–	–	–	–	–	–	–	–	0.13	–	–	–	–	–
Cl	–	–	–	–	–	–	–	–	–	0.11	–	–	–	–	–
Sum	91.05	95.90	95.19	95.14	95.65	96.15	95.28	95.95	89.98	86.69	85.76	87.35	83.18	88.36	89.21
100 Mg/ Mg+Fe^{tot}	70.2	69.3	61.9	62.3	25.6	46.9	32.9	–	–	85.7	77.9	52.1	29.3	16.1	89.1
Basis	22 oxygens								Si = 8.000	28 oxygens			20 cations		22 oxygens
Si	5.062	5.301	5.294	5.442	5.772	5.840	5.811	5.828	8.000	7.793	6.962	7.134	5.772	5.292	7.025
Ti	0.049	0.863	0.968	0.847	0.358	0.396	0.363	–	–	–	–	–	0.023	0.023	0.011
Al	3.171	2.593	2.554	2.409	2.174	1.958	2.028	6.146	–	0.492	2.277	2.893	4.457	5.313	0.029
Fe	1.949	1.460	1.771	1.825	3.955	2.763	3.312	0.114	–	1.645	2.341	4.402	6.647	7.494	0.790
Mn	–	–	–	–	0.166	0.268	0.555	–	–	0.028	–	0.024	0.135	0.347	–
Mg	4.590	3.297	2.879	3.018	1.360	2.438	1.626	–	3.897	9.886	8.276	4.788	2.753	1.436	7.024
Ca	0.050	0.044	0.027	–	–	0.028	0.016	–	–	0.057	0.043	0.148	0.037	–	–
K	0.810	1.755	1.855	1.839	1.886	1.952	1.966	1.935	1.994	–	–	0.061	0.051	–	–
Na	0.052	0.153	0.080	0.091	0.106	0.137	0.144	0.085	–	–	–	–	0.127	0.096	–
SO_3	–	–	–	–	–	–	–	–	–	0.018	–	–	–	–	–
Cl	–	–	–	–	–	–	–	–	–	0.038	–	–	–	–	0.015
Σ cations	15.733	15.466	15.428	15.471	15.777	15.780	15.821	14.108	13.891	19.957	19.899	19.450	–	–	14.894

Key to Table 5

Analyses 1–9 are micas

The basic complex

1. WB 154: late stage K-deficient colourless phlogopite.
2. WB 156: large grain of titanphlogopite.
3. WB 151: titanbiotite – rim on magnetite.
4. WB 153: late green biotite.

The northern complex

5. WB 7: centre of large biotite grain.

The nepheline syenite complex

6. WB 273: brown biotite in biotite aggregate.
7. WB 82: brown biotite in aggregate.
8. WB 300: colourless interstitial muscovite.
9. WB 253: colourless taeniolite needle in quartz.

Analyses 10–14 are chlorites

The basic complex

10. WB 154: talc-chlorite.
11. WB 154: chlorite (penninite).
12. WB 153: chlorite (diabatite).

The northern complex

13. WB 7: chlorite (brunsvigite).
14. WB 7: chlorite (ripidolite).

Analysis 15 is serpentine

15. WB 156: serpentine after olivine.

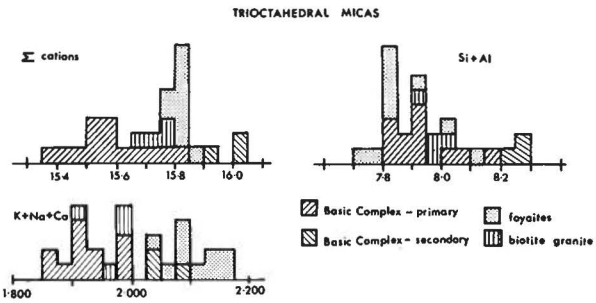

Fig. 26. Histograms showing site populations for Werner Bjerge trioctahedral micas, calculated on the basis of 22 oxygens. The basic complex has an average for total cations of 15.55, the granites 15.75 and the foyaites 15.83, while the sum of K + Na + Ca rises from 1.92 to 1.97 to 2.10 in the same sequence.

chlorite in the biotite granite. Representative analyses of these phases are presented in Table 5, where they are classified after Deer et al. (1962).

In this work, we have chosen to recalculate the mica (except taeniolite) analyses on the basis of 44 charges with all Fe as FeO. Chlorites are arbitrarily normalised on the basis of 20 cations and, where possible, 56 charges per formula unit. Taeniolite is recalculated with Si = 8.000 and charge balancing then leads to an estimate of its Li content. Many complications in the sheet silicate crystal chemistry, which combine with limitations in the microprobe capabilities, make all procedures of this nature less than ideal, but alternative schemes (e.g. as proposed by Ludington 1974, Hildreth 1977 and Stern 1979) are not clearly to be preferred.

Several features (shown in Fig. 26) suggest that our adopted procedure is reasonably satisfactory: micas show consistent differences between rock-types, the cation sums are in all cases below the ideal 16.0 and micas from the basic complex have the largest apparent cation deficiencies. However, biotites from the foyaites show the impossible feature of excess interlayer cations which may be accounted for by the presence of Fe^{3+}, undetermined additional constituents (e.g. Li, Ba) or simply by slight overestimation of Na_2O. Despite other differences, all micas have similar amounts of Si+Al, often below 8.00 suggesting that tetrahedral Fe^{3+} is in fact present, thus accounting for the brown colour. Green micas on the other hand have characteristically an excess of Si+Al, even after oxidation and thus have a minimal cation deficiency.

4.4.2 The basic complex. – The deep red-brown micas in the gabbros have 100 Mg/Mg+Fe ratios in the range 55–82 and are highly titaniferous with up to 8.8% TiO_2 (Table 5). The earliest-formed micas are generally the most Ti- and Fe-rich, while the later are more Ti-poor and Mg-rich. Each rock has its own Ti-enrichment level (Fig. 27). The number of apparent vacancies in the octahedral positions is highest in the most Ti-rich micas, suggesting either that Ti is involved in a vacancy substitution, or that these micas have the least amounts of Fe^{3+}.

The secondary sheet silicates in the basic rocks are Mg-rich types: talc, talc-chlorite and penninite and diabantite with 100 Mg/Mg+Fe = 52–86. They all contain less than 0.5% TiO_2 and there is no indication that these phases contain any substantial amounts of

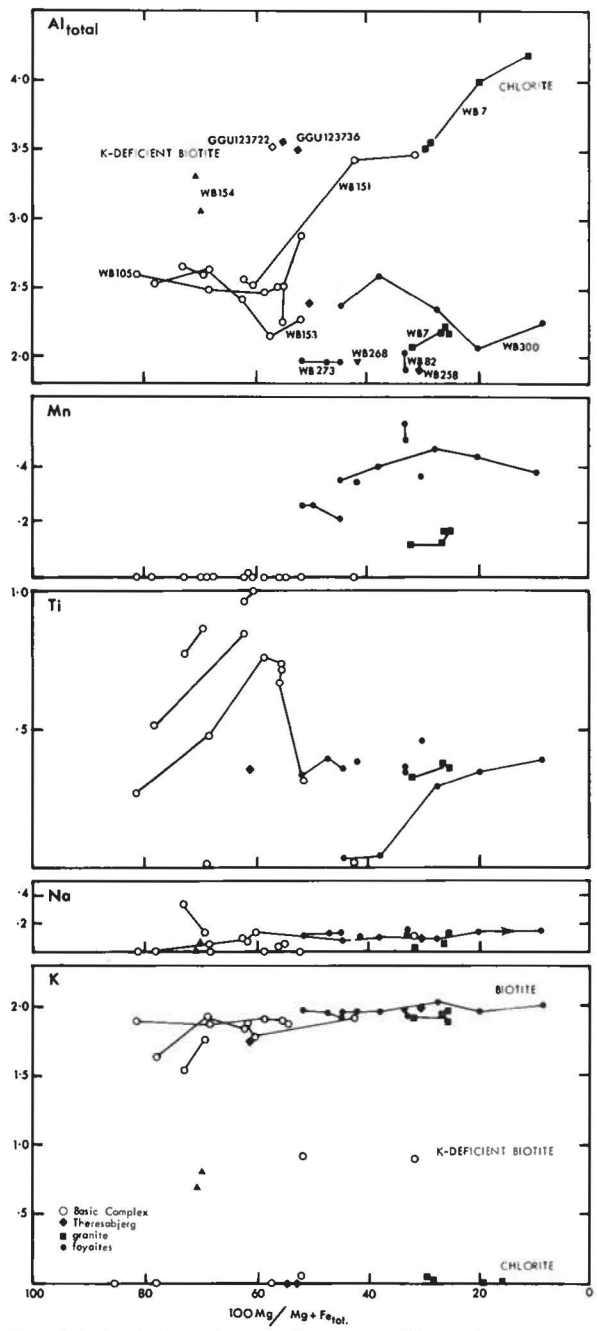

Fig. 27. Variation diagram for sheet silicates in terms of Mg/Mg + Fe^{total}. Lines connect analyses from the same rock.

Fe^{3+}. For the mixed layer biotite-chlorites the sum of Na+K+Ca is in the range 0.9–1.5 indicating that every second to every fourth layer is chloritic or vermiculitic in type.

The titaniferous micas from the basic complex are essentially similar to those described by Brooks & Platt (1975) from the inclusions of kaersutite gabbro in the late dyke swarm of Kangerdlugssuaq. Similar micas are known from basic units associated with other alkaline complexes, e.g. Monchique (Rock 1978) and the Trans-Pecos province (Baker & Hodges 1977).

4.4.3 The northern complex. – In the biotite granite the main mafic silicate is a yellow to dark dirty-brown iron-rich biotite with 100 Mg/Mg+Fe = 25–31 (Table 5). This rock contains correspondingly Fe-rich chlorites varying from brunsvigite to ripidolite, with 100 Mg/Mg+Fe = 16–29. These phases have relatively low manganese contents (Fig. 27). Thus, the extreme enrichment in MnO observed in the mafic minerals of the alkali granite is not paralleled in the biotite granite.

4.4.4 The nepheline syenite complex. – The yellow to dark brown biotites in these rocks are iron-rich, with 100 Mg/Mg+Fe = 8–49, complementary to those in the basic rocks (Table 5, Fig. 27). They generally have lower Ti contents than those in the basic rocks, and they contain considerable amounts of MnO (1.56–4.06%). The highest Mn content is observed in the biotites from the most differentiated foyaite (WB 82). Biotites do not generally contain more than 2% MnO, but up to 5.2% MnO has been reported in biotites from Shonkin Sag (Nash & Wilkinson 1970).

On the basis of the present data, no general evolutionary trend in the biotites, corresponding to the increasing alkalinity of the foyaites, can be distinguished. However, the rocks appear to show individual biotite trends very similar to those observed in the basic complex. Thus in one of the more primitive foyaites (WB 300) the five analysed biotites form a sequence in which decreasing Ti is associated with a decrease in total Fe and a rise in Si, Al and Mg (Fig. 27).

In addition to biotite, two of the foyaites (WB 300 and WB 258) contain small amounts of very pure secondary muscovite. Even these analyses show excess K+Na, possibly indicating some Li.

The narsarsukite pegmatite contains the rare Li-mica taeniolite, $K_2Li_2Mg_4Si_8O_{20}F_4$. The analyses show that the actual compositions are quite close to the theoretical formula (Table 5). When the analyses are recalculated on the basis of 8 Si atoms per formula unit, charge balance calculations result in 2.1–2.2 Li atoms per formula unit, corresponding to approx. 3.8% Li_2O. An assumed fluorine content of 4 atoms per formula unit leads to calculated fluorine contents of 9.2–9.3% F. With correction for $O = F_2$ the analyses thereafter sum to 97.2–99.6%, which is acceptable.

Hitherto taeniolite has only been recorded from the narsarsukite pegmatites at Narssârssuk in South Greenland (Bøggild 1953), from Magnet Cove, Arkansas (Miser & Stevens 1938) where it occurs in cherts some distance from the igneous contact, and from the Kola Peninsula (Vlasov 1966).

4.4.5 Comparison of amphiboles and micas. – As earlier noted there is an evident antipathetic relation between the occurrence of amphibole and mica in all rock groups. Table 6 compares the amphiboles and micas in the basic rocks and in the nepheline syenites. The chemical analogies between the two mineral groups are obvious. The granites are too different for a meaningful comparison.

4.5 Feldspars, feldspathoids and zeolites

4.5.1 Introduction. – The distribution of feldspars, feldspathoids and zeolites among the investigated samples is listed in Table 2. The analyses include semiquantitative determinations for Ba but not Sr or Rb. The extreme range of feldspar compositions, from calcic bytownite to alkali feldspar, covered by these rocks is illustrated in Fig. 28. The feldspathoids and zeolites from the nepheline syenites include nepheline, sodalite, cancrinite, analcime, thompsonite and possibly gonnardite.

The kaersutite-bearing mafic inclusions from Theresabjerg occasionally have interstitial alkali feldspar, but contain no feldspathoids or cumulus feldspar. Only the samples from the Werner Bjerge complex are commented upon in the following.

Table 6. Comparison of amphiboles and biotites.

	Basic complex		Nepheline syenite complex	
	amphiboles	phlog.-biotites	amphiboles	biotites
100 Mg/Mg + Fe + Mn	44.5–96.5	42.3 –81.2	15.9 –36.5	8.0 –49.0
TiO_2, wt %	0–6.45	0.13 – 8.84	0.23 – 2.05	0.27 – 3.82
Ti atoms per formula unit	0– 0.724	0.014– 1.004	0.028– 0.243	0.033– 0.462
MnO, wt %	0– 0.33	0	2.61 – 4.30	1.56 – 4.06
Mn atoms per formula unit	0– 0.043	0	0.340– 0.559	0.211– 0.555

Note that these amphiboles and biotites do *not* coexist but, on the contrary, proxy for each other.

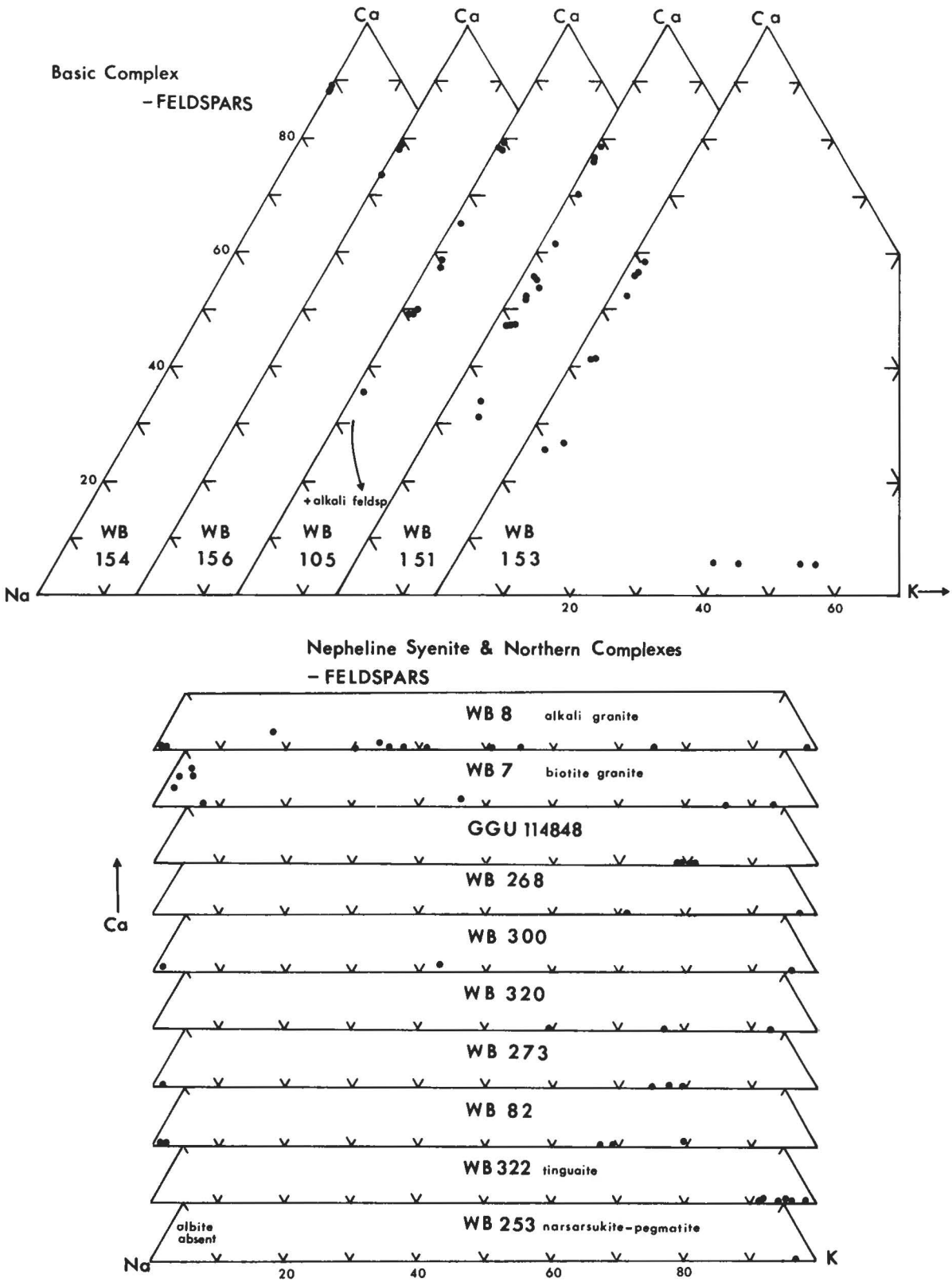

Fig. 28. Feldspar variation in terms of Na–K–Ca for the analysed points (i.e. additional variation may well be present). For foyaite WB 258 no analyses are available.

Table 7. Representative analyses of feldspars from Werner Bjerge.

	1	2	3	4	5	6	7	8	9	10	11
SiO_2	45.22	47.87	53.29	58.78	63.66	66.02	65.93	64.39	67.83	63.27	63.69
TiO_2	–	–	0.21	0.13	0.20	–	–	–	–	–	–
Al_2O_3	34.30	32.60	28.89	25.78	18.69	21.05	19.24	19.00	20.32	18.04	18.53
FeO	0.31	0.39	0.36	0.43	0.20	0.22	0.16	–	–	–	–
MgO	0.25	0.12	0.17	0.11	–	–	–	–	–	–	–
CaO	18.05	15.68	10.66	7.06	0.16	1.36	0.26	–	0.15	–	–
K_2O	–	0.13	0.49	0.85	15.67	0.39	7.89	12.43	0.21	16.26	16.17
Na_2O	1.20	2.31	5.13	6.97	0.74	10.17	5.99	3.29	11.29	0.43	0.68
Sum	99.33	99.11	99.21	100.10	99.32	99.21	99.47	99.11	99.80	98.00	99.07
					Cations on basis of 32 oxygens						
Si	8.403	8.854	9.731	10.525	11.864	11.672	11.911	11.877	11.873	11.964	11.911
Ti	–	–	0.029	0.018	0.028	–	–	–	–	–	–
Al	7.512	7.107	6.218	5.440	4.104	4.386	4.097	4.129	4.191	4.021	4.084
Fe	0.048	0.061	0.055	0.064	0.031	0.033	0.025	–	–	–	–
Mg	0.068	0.034	0.046	0.030	–	–	–	–	–	–	–
Ca	3.593	3.106	2.086	1.354	0.031	0.258	0.050	–	0.028	–	–
K	–	0.031	0.114	0.193	3.724	0.089	1.819	2.925	0.046	3.921	3.858
Na	0.432	0.828	1.817	2.419	0.269	3.485	2.098	1.178	3.832	0.158	0.246
An	89.3	78.3	51.9	34.1	0.8	6.7	1.2	–	0.7	–	–
Ab	10.7	20.9	45.2	61.0	6.7	90.9	52.9	28.7	98.1	3.9	6.0
Or	–	0.8	2.8	4.9	92.5	2.3	45.9	71.3	1.2	96.1	94.0

Key to Table 7

The basic complex

1. WB 154: core of plagioclase in mafic cumulate.
2. WB 105: core of plagioclase in syenogabbro.
3. WB 151: intermediate zone in plagioclase in gabbro.
4. WB 151: rim of plagioclase in gabbro.
5. WB 105: interstitial K-feldspar in syenogabbro.

The northern complex

6. WB 7: plagioclase in biotite granite.
7. WB 7: K-feldspar in biotite granite.

The nepheline syenite complex

8. WB 268: optically homogeneous K-feldspar in nepheline syenite.
9. WB 300: albitic phase of perthite in nepheline syenite.
10. WB 300: K-rich phase of perthite in previous.
11. WB 322: K-feldspar phenocryst in tinguaite.

4.5.2 The basic complex. – According to Bearth (1959, table 1 and pp. 15–19), feldspars are absent from the early pyroxenites, whereas the gabbroic rocks contain normally zoned plagioclase with cores of bytownite optically determined to be in the range $An_{89} - An_{80}$. The syeno-gabbroic rocks contain plagioclase of predominantly labradorite to andesine compositions with interstitial K-feldspar.

The present feldspar analyses from the gabbroic rocks (Fig. 28, Table 7) are in close agreement with Bearth's optical determinations. Thus the core compositions of the cumulus feldspars in the present samples range from An_{89} to An_{79}. The most calcic plagioclase occurs in the mafic cumulate (WB 154) but otherwise no systematic cryptic variation can be detected on the basis of the present data. Gabbro WB 153 has a considerably more evolved plagioclase (cores An_{58}) than the other rocks. Except for a few intermediate compositions, the calcic cumulus plagioclase is sharply bounded against the intercumulus plagioclase which has compositions ranging down to An_{25}. Small amounts of interstitial K-feldspar occur in two of the more evolved gabbros (WB 153 & WB 105). The intercumulus plagioclase and K-feldspar contain appreciable amounts of Ba (Table 7).

No feldspathoids have been observed in the mafic rocks from the complex either by Bearth (1959, p. 15) who examined more than fifty samples, or in the present work.

4.5.3 The northern complex. – Plagioclase is a rare mineral in the northern complex, having been observed only once by Bearth (1959, p. 28). However, the biotite granite (WB 7) investigated here is a two feldspar rock in which large grains of sodic plagioclase (An_5–An_7) coexist with an optically homogeneous alkali feldspar with a composition around $Or_{46}Ab_{53}An_1$ (Fig. 28, Table 7). Such an association indicates crystallisation at around 620°C (Stormer 1975, Powell & Powell 1977).

The alkali granite (WB 8) contains microperthite with a bulk composition in the range Or_{25} to Or_{50} (broad beam analyses) as well as individual grains of almost pure albite (Ab_{98}) and K-feldspar (Or_{98}).

Table 8. Representative analyses of nepheline, sodalite, cancrinite, analcime and zeolites from the nepheline syenite complex of Werner Bjerge.

mineral	1	2 nepheline	3	4 sodalite	5 cancrinite	6 analcime	7 zeolites	8
SiO_2	45.20	44.07	43.25	36.61	36.58	52.13	35.84	43.22
Al_2O_3	32.85	32.95	34.69	32.19	28.59	24.26	30.08	28.64
Fe_2O_3	0.67	0.79	0.21	–	0.23	–	0.51	0.06
CaO	–	0.64	0.11	–	4.61	0.23	12.74	4.85
K_2O	5.58	5.78	7.09	–	–	1.04	–	0.09
Na_2O	15.60	15.85	15.91	24.30	19.34	12.73	4.06	10.11
SO_3	–	–	–	0.49	0.09	–	–	–
Cl	–	–	–	7.35	–	–	–	–
Sum	99.80	100.08	101.26	100.94	89.44	90.39	83.23	86.95
basis		32 oxygens		21 oxygens	12 (Si + Al)	7 oxygens	20 oxygens	
Si	8.627	8.459	8.235	5.911	6.236	1.950	4.999	5.522
Al	7.389	7.453	7.785	6.115	5.734	1.070	4.946	4.303
Fe^{3+}	0.096	0.114	0.031	–	0.030	–	0.054	–
Ca	–	0.131	0.023	–	0.842	0.009	1.904	0.660
K	1.359	1.416	1.723	–	–	0.050	–	0.015
Na	5.771	5.897	5.872	7.598	6.381	0.923	1.098	2.500
SO_3	–	–	–	0.058	0.011	–	–	–
Cl	–	–	–	2.035	–	–	–	–
Ne	72.9	74.2	72.9	–	–	–	–	–
Ks	19.1	19.8	23.8	–	–	–	–	–
Qz	8.0	6.0	3.3	–	–	–	–	–

Key to Table 8

The nepheline syenite complex

1. WB 82: large nepheline grain in nepheline syenite.
2. WB 322: nepheline in phenocryst in tinguaite.
3. WB 322: nepheline in groundmass of tinguaite.
4. WB 268: sodalite in nepheline syenite.
5. WB 268: cancrinite, possibly after nepheline, in nepheline syenite.
6. WB 300: analcime, possibly after nepheline, in nepheline syenite.
7. WB 82: thompsonite, interstitial, in nepheline syenite.
8. WB 300: gonnardite (?), apparently replacing nepheline in nepheline syenite.

4.5.4 The nepheline syenite complex. – Alkali feldspar and feldspathoids are quantitatively the most important minerals in the nepheline syenites. Feldspathoids, largely nepheline and sodalite sometimes accompanied by analcime and cancrinite, may constitute up to 30–40% of these rocks. The Na-Ca-zeolites thompsonite and gonnardite (Table 8) occur interstitially and replace nepheline.

The homogeneous alkali feldspars generally have compositions in the range Or_{70-80}. This is considerably more potassic than any of the feldspars of the Kangerdlugssuaq syenites (Kempe & Deer 1970). No significant zonation was observed, and feldspar phenocrysts, such as those in the Kangerdlugssuaq intrusion, have not been encountered.

The tinguaite (WB 322, Fig. 28, Table 7) contains phenocrysts of a very potassic feldspar (Or_{95}) coexisting with phenocrysts of Ca-rich nepheline (0.64% CaO) and sodalite, whereas the groundmass contains two feldspars, one sodic (Ab_{91}) and the other potassic (Or_{95}), and a Ca-poor nepheline (0.11% CaO). The amount of excess SiO_2 in the nephelines indicates that the phenocryst assemblage in the tinguaite equilibrated at around 770°C and the groundmass nepheline at about 700°C (Hamilton 1961).

Compared to the tinguaite, the nephelines of the foyaites generally have a slightly higher excess of SiO_2 indicative of crystallisation temperatures in the range 900 to 800°C. Unfortunately, the Sr content of the nephelines was not determined. Bearth (1959, p. 58) reports a Sr content of nearly 1% for nepheline from a foyaite.

The analyses of sodalite, cancrinite, analcime and zeolites given in Table 8 are unremarkable except that most sodalite analyses show small amounts of S, in the range 0–0.5%, rising to 0.6–1.9% S in phenocryst cores in the tinguaite.

The quartz-bearing narsarsukite pegmatite contains chessboard-twinned microcline (Or_{97}) as its only feldspar.

Table 9. Representative analyses of Fe–Ti–Mn oxide minerals from Werner Bjerge.

mineral	1 mag.	2 ilm.	3 mag.	4 ilm.	5 mag.	6 pyph.	7 mag.	8 pyph.
TiO_2	6.20	50.31	13.91	51.91	3.60	51.33	6.99	50.61
Al_2O_3	3.92	0.13	3.28	0.23	0.35	0.10	0.62	0.24
Cr_2O_3	0.16	–	0.27	–	–	–	–	–
V_2O_3	1.12	–	0.77	–	–	–	0.34	–
FeO	83.62	46.76	76.34	43.07	89.47	4.92	81.38	9.25
MnO	0.30	1.39	0.40	0.84	3.32	40.69	4.13	36.47
MgO	0.88	0.77	2.38	4.55	–	–	–	–
CaO	–	–	0.10	0.08	–	–	–	0.10
sum	96.20	99.36	97.45	100.68	96.74	97.04	93.46	96.67
Fe_2O_3	52.58	4.78	39.49	6.06	63.80	–	53.64	0.90
FeO	36.30	42.46	40.81	37.62	32.06	4.92	33.12	8.45
New sum	101.45	99.84	101.40	101.29	103.13	97.04	98.84	96.77
cations on basis of 24 cations 32 oxygens (magnetite) and 4 cations 6 oxygens (ilmenite and pyrophanite)								
Ti	1.368	1.906	3.025	1.883	0.805	1.998	1.621	1.975
Al	1.356	0.008	1.118	0.013	0.123	0.006	0.225	0.015
Cr	0.042	–	0.083	–	–	–	–	–
V	0.255	–	0.155	–	–	–	0.083	–
Fe^{3+}	11.611	0.181	8.593	0.220	14.268	–	12.449	0.035
Fe^{2+}	8.909	1.789	9.871	1.518	7.969	0.213	8.542	0.367
Mn	0.075	0.059	0.098	0.034	0.836	1.783	1.079	1.603
Mg	0.385	0.058	1.026	0.327	–	–	–	–
Ca	–	–	0.031	0.004	–	–	–	0.006
Hm	–	4.82	–	6.76	–	0.00	–	4.55
Usp.	16.40	–	36.30	–	5.14	–	14.81	–

Key to Table 9

The basic complex

1. WB 153: cumulus magnetite grain with ilmenite exsolution in gabbro.
2. WB 153: ilmenite lamellae in above.
3. WB 156: cumulus magnetite in gabbro.
4. WB 156: cumulus ilmenite in gabbro.

The northern complex

5. WB 8: magnetite in alkali granite.
6. WB 8: pyrophanite in alkali granite.

The nepheline syenite complex

7. WB 300: large euhedral magnetite.
8. WB 82: pyrophanite.

4.6 Fe-Ti-Mn oxides

4.6.1 Introduction. – The distribution of oxide minerals among the investigated samples is listed in Table 2; they include titanomagnetite, ilmenite and, in the alkali granite and some of the more evolved nepheline syenites, pyrophanite, the Mn analogue of ilmenite. No oxides were observed in the narsarsukite pegmatite. Representative analyses are given in Table 9.

4.6.2 The basic complex. – As is normal in plutonic rocks, the Fe-Ti oxides exhibit a range of subsolidus exsolution textures (e.g. Haggerty 1976). The titanomagnetite crystals least modified by ilmenite exsolution have approximately 24% TiO_2 (= 73% ulvöspinel) and this is regarded as a minimum value for the original composition. Relatively large ilmenite grains intergrown with titanomagnetite grains give calculated equilibrium temperatures of 750–820°C and f_{O_2} around the FMQ buffer curve, while ilmenite lamellae in host magnetite give 540–610°C around the NNO buffer curve when calculated after Powell & Powell (1977). These temperatures are not thought to reflect magmatic conditions, but rather blocking temperatures for the various exsolution processes.

Both oxides exhibit ranges of minor elements within the limits given by Haggerty (1976) and show only minor variations. MnO in ilmenites varies from 0.8–1.4% while MnO in titanomagnetites is below 1% (Fig. 29). Cr_2O_3 in the titanomagnetites varies from 1.47% in the mafic cumulate (WB 154) to zero in the most evolved gabbro (WB 151). The titanomagnetites from the Theresabjerg inclusions have no detectable MnO or Cr_2O_3.

Table 10. Representative analyses of Ti garnets, narsarsukite, Mn-pectolite and kupletskite from Werner Bjerge.

	1	2	3	4	5	6
SiO_2	34.05	31.38	61.82	61.92	53.27	34.80
TiO_2	3.39	8.19	11.70	15.33	–	6.34
Al_2O_3	1.04	2.12	0.89	0.47	–	1.72
V_2O_5	0.49	0.38	–	–	–	–
FeO	24.61	22.27	5.61	3.74	–	9.69
MnO	0.75	0.57	0.15	–	4.39	22.34
MgO	0.22	0.28	–	–	–	0.57
CaO	32.49	31.85	–	–	28.94	0.75
K_2O	–	–	0.28	0.24	0.07	6.27
Na_2O	–	–	15.31	15.27	8.80	3.23
Nb_2O_5	–	–	–	–	–	5.16*
Sum	97.04	97.04	95.76	96.97	95.46	90.87
Fe_2O_3	26.23	21.42	4.51	2.31	–	–
FeO	1.00	2.99	1.55	1.66	–	–
new sum	99.66	99.18	96.21	97.20	–	–
Basis	8 cations 12 oxygens		7 cations 11 oxygens		17 oxygens	Si + Al = 8.000
Si	2.881	2.671	4.062	4.048	6.044	7.557
Ti	0.215	0.524	0.578	0.754	–	1.030
Al	0.104	0.213	0.069	0.036	–	0.443
V	0.033	0.026	–	–	–	–
Fe^{2+}	1.670	1.372	0.223	0.114	–	1.759
Fe^{2+}	0.071	0.213	0.085	0.091	–	
Mn	0.053	0.041	0.009	0.020	0.421	4.101
Mg	0.027	0.036	–	–	–	0.183
Ca	2.945	2.904	–	–	3.518	0.170
K	–	–	0.023	0.020	0.009	1.733
Na	–	–	1.950	1.986	1.936	1.355
Nb	–	–	–	–	–	0.508

Key to Table 10

The nepheline syenite complex

1. GGU 114848: Ti-garnet (melanite) in nepheline syenite – TiO_2-poor variety.
2. GGU 114848: Ti-garnet (melanite) in nepheline syenite – analysis richest in TiO_2.
3. WB 253: core of narsarsukite, $Na_2(Ti, Fe)Si_4O_{11}$, in pegmatite. Contains c. 0.5% ZrO_2.
4. WB 253: rim of narsarsukite grain, as previous. ZrO_2 not detectable.
5. WB 253: Mn pectolite, $Na_2\ (Ca, Mn)_4\ Si_6\ O_{16}\ (OH)_2$, enclosed in feldspar.
6. WB 322: fine-grained kupletskite in analcime in groundmass of tinguaite. Ideal formula after Macdonald & Saunders (1973) is $(K, Na, Ca)_3(Fe, Mn, Mg)_7(Ti, Nb)_2(Si, Al)_8(O, OH)_{31}$.

* semi-quantitative analysis.

terms of the elements determined, its composition is similar to analyses quoted by Vlasov (1966) and Segalstad & Larsen (1978). An analysis of chevkinite was also presented by Brooks & Rucklidge (1976) from Kangerdlugssuaq where it is an almost ubiquitous constituent of the nordmarkites and granites.

Apart from zircon which occurs in several of the samples (Table 2), zirconosilicates are difficult to identify on the basis of semi-quantitative analyses due to the extensive substitution which occurs. The foyaite GGU 114848 contains a mineral which resembles chemically a titaniferous variety of hjortdahlite. The foyaite WB 320 contains a mineral with a rosenbuschite-like chemistry and the tinguaite (WB 322) contains a Na-Zr silicate for which no comparable analysis is known. All the zirconosilicates occur interstitially as small grains which are colourless in thin section and have a high birefringence.

4.7.10 Mn pectolite. – A characteristic but hitherto unreported mineral from the narsarsukite pegmatite (WB 253) is Mn pectolite (Table 10). It occurs as small dirty looking grains with clear centres, often enclosed in feldspar. At Igdlutalik, South Greenland, the narsarsukite occurs together with a Mn-free pectolite (Upton et al. 1976).

4.7.11 Calcite. – Late-stage carbonates are widespread throughout the Werner Bjerge complex, both disseminated in the rocks and as vein fillings. Calcite, siderite, strontianite and baryte have been reported by Bearth (1959), the last two carbonates occurring as vein fillings

in the foyaites. In the rocks studies here, only calcite with minor amounts of other elements has been observed. The calcite in the gabbro WB 153 contains 1.2% MnO and traces of Fe and Mg. Sparse interstitial carbonate in the foyaite WB 268 is almost pure calcite. In the narsarsukite pegmatite (WB 253), the calcite contains about 0.5% SrO.

Conclusions

The Werner Bjerge complex is of interest due to its complexity and its economic significance, mineralisations being connected both with this specific complex, and with Tertiary plutonism of the area in general.

The complex consists of a diverse suite of rock types ranging from mafic and ultramafic to alkali syenites, granites and nepheline syenites. The geochemistry of the rocks (Bearth 1959) shows a coherence indicative of a comagmatic origin for most units of the intrusion, and the mineralogy of the rocks as described here strongly supports this view. Thus, for example, the pyroxene cores in different units of the nepheline syenite complex form a single trend (Fig. 20) which can be directly extrapolated to the pyroxene trend for the basic complex, although there is a gap between them. The position of this pyroxene trend suggests that the rocks evolved under moderately high oxygen fugacities. Furthermore, a remarkable feature of the minerals of the various rock units (with the exception of the biotite granite) is the unusually high manganese content in the mafic silicates and oxides.

The molybdenum deposit at Malmbjerg is connected with an alkali granite intrusion, and the mineralisation is enriched in Fe, Mn, Ti, Zr, Nb, Zn, Mo, W, Li and F (Bearth 1959). Viewed in this perspective it can be concluded that in fact all the rocks of the complex show signs of the mineralising potential of the magma in a) the occurrence of a number of accessory minerals, e.g. pyrochlore (Nb), chevkinite (REE) zirconosilicates and taeniolite (Li, F), and b) the high concentrations of Mn, both dispersed in the rock-forming mafic silicates and oxides (where pyrophanite occurs), and also in manganese minerals such as kupletskite and mangan-pectolite. These features may prove useful in future assessments of mineralisation potentials of other igneous complexes in the province.

Syenitic and granitic rocks are widespread in the East Greenland Tertiary. The Kangerdlugssuaq intrusion about 500 km to the south of Werner Bjerge (Fig. 1) shows a striking mineralogical similarity to the Werner Bjerge complex. Although no basic complex is exposed at Kangerdlugssuaq, associated dykes contain gabbroic cumulate inclusions (Brooks & Platt 1975) which are mineralogically very similar to the cumulates from Werner Bjerge and Theresabjerg described here, and indicate that a similar body is present at no great depth.

In both the Kangerdlugssuaq and Borgtinderne complexes there is isotopic evidence for crustal contamination as an important modifying factor in the evolution of the rocks (Pankhurst et al. 1976, Brown et al. 1978). The unusually broad spectrum of mineral variation in the Werner Bjerge complex represents a protracted process of magmatic evolution which may reflect both crystal fractionation and contamination, the extent of which has to be established by future isotopic studies.

Acknowledgements

We thank the following institutions and persons: The Geological Museum, Copenhagen, made the material from Bearth's collection available for study. The Research School of Earth Sciences, Canberra, provided working facilities for LML and AKP, and Nick Ware assisted with the microprobe work. Haldis Bollingberg made the optical spectrographic determinations of lithium. The results for the GGU material are published with the permission of the Director of the Geological Survey of Greenland.

References

Barker, D. S. & Hodges, F. N. 1977. Mineralogy of intrusions in the Diablo Plateau, northern Trans-Pecos magmatic province, Texas and New Mexico. – Bull. geol. Soc. Am. 88: 1428–1436.

Bearth, P. 1959. On the alkali massif of the Werner Bjerge in East Greenland. – Meddr Grønland 153 (4): 62 pp.

Bondam, J. & Brown, H. 1955. The geology and mineralisation of the Mesters Vig Area, East Greenland. – Meddr Grønland 135 (7): 40 pp.

Borley, G. D. 1963. Amphiboles from the Younger Granites of Nigeria. Part 1. Chemical classification. – Miner. Mag. 33: 358–376.

Brooks, C. K. 1973. The Tertiary of Greenland – a volcanic and plutonic record of continental break-up. – Mem. Am. Ass. Petrol. Geol. 19: 150–160.

Brooks, C. K. & Gill, R. C. O. in press. Compositional variation in the pyroxenes and amphiboles of the Kangerdlugssuaq intrusion, East Greenland: Further evidence for the crustal contamination of a syenite magma. – Miner. Mag.

Brooks, C. K. & Platt, R. G. 1975. Kaersutite-bearing gabbroic inclusions and the late dike swarm of Kangerdlugssuaq, East Greenland. – Miner. Mag. 40: 259–283.

Brooks, C. K. & Rucklidge, J. C. 1976. Tertiary peralkaline rhyolite dikes from the Skaergaard area, Kangerdlugssuaq, East Greenland. – Meddr Grønland 197 (3): 24 pp.

Brown, P. E., Brown, R. D., Chambers, A. D. & Soper, N. J. 1978. Fractionation and assimilation in the Borgtinderne Syenite, East Greenland. – Contr. Miner. Petrol. 67: 25–34.

Bøggild, O. B. 1953. The mineralogy of Greenland. – Meddr Grønland 149 (3): 442 pp.

Carmichael, I. S. E., Turner, F. J. & Verhoogen, J. 1974. Igneous Petrology. – McGraw Hill, New York: 739 pp.

Craig, J. R. & Scott, S. D. 1974. Sulfide phase equilibria. – In: Ribbe, P. H. (ed.). Short course notes. Vol. 1. Sulfide Mineralogy, Miner. Soc. Am., Washington D.C.: CS-1 to CS-110.

Deer, W. A. 1976. Tertiary igneous rocks between Scoresby Sund and Kap Gustav Holm, East Greenland. – In:

Escher, A. & Watt, W. S. (eds). Geology of Greenland. – The Geological Survey of Greenland, Copenhagen: 430–458.

Deer, W. A., Howie, R. A. & Zussman, J. 1962. Rock-forming minerals. Vol. 3. Sheet silicates. – Longman, London: 270 pp.

Deer, W. A., Howie, R. A. & Zussman, J. 1963. Rock-forming minerals. Vol. 2. Chain silicates. – Longman, London: 379 pp.

Deer, W. A., Howie, R. A. & Zussman, J. 1978. Rock-forming minerals. Vol. 2A (2nd ed.). Single chain silicates. – Longman, London: 668 pp.

Engell, J. 1975. The Kap Parry complex, central East Greenland. – Rapp. Grønlands geol. Unders. 75: 103–106.

Ferguson, A. K. 1977. The natural occurrence of aegirine-neptunite solid solution. – Contr. Miner. Petrol. 60: 247–253.

Frisch, T. 1970. Chemical variations among amphiboles of Shefford Mountain, a Monteregian intrusion in southern Quebec. – Can. Mineralogist 10: 553–570.

Gleadow, A. J. W. & Brooks, C. K. 1979. Fission track dating, thermal histories and tectonics of igneous intrusions in East Greenland. – Contr. Miner. Petrol. 71: 45–60.

Haggerty, S. E. 1976. Opaque mineral oxides in terrestrial igneous rocks. – In: Rumble, D. III (ed.). Short course notes. Vol. 3. Oxide minerals. Miner. Soc. Am., Washington D.C.: Hg-101 to Hg-300.

Hamilton, D. L. 1961. Nephelines as crystallization temperature indicators. – J. Geol. 69: 321–329.

Hildreth, E. W. 1977. The magma chamber of the Bishop Tuff: gradients in temperature, pressure and compositions. – (Ph. D. Thesis). University of California, Berkeley: 328 pp.

Huckenholz, H. G., Schairer, J. F. & Yoder, H. S. Jr. 1969. Synthesis and stability of ferri-diopside. – In: Miner. Soc. Am. Spec. Publ. 2: 163–177.

Kapp, H. 1960. Zur Petrologie der Subvulkane zwischen Mesters Vig und Antarctic Havn (Ost-Grönland). – Meddr Grønland 153 (2): 203 pp.

Kempe, D. R. C. & Deer, W. A. 1970. Geological investigations in East Greenland. Part IX. The mineralogy of the Kangerdlugssuaq intrusion, East Greenland. – Meddr Grønland 190 (3): 95 pp.

Kempe, D. R. C., Deer, W. A. & Wager, L. R. 1970. Geological investigations in East Greenland. Part VIII. The petrology of the Kangerdlugssuaq intrusion, East Greenland. – Meddr Grønland 190 (2): 49 pp.

Kirchner, G. 1964. Die molybdänlagerstätte des Erzberges bei Mesters Vig, Ostgrönland. – Berg. Huttenmänn. Mh. (Wien) 109: 162.

Larsen, L. M. 1976. Clinopyroxenes and coexisting mafic minerals from the alkaline Ilímaussaq intrusion. – J. Petrology 17: 258–290.

Larsen, L. M. 1981. Sector zoned aegirine from the Ilímaussaq alkaline intrusion, South Greenland. – Contr. Miner. Petrol. 76: 285–291.

Leake, B. E. 1978. Nomenclature of amphiboles. – Miner. Mag. 42: 533–563.

Ludington, S. 1974. The biotite-apatite geothermometer revisited. – Am. Miner. 63: 551–553.

MacDonald, R. & Saunders, M. J. 1973. Chemical variation in minerals of the astrophyllite group. – Miner. Mag. 39: 97–111.

Miser, H. D. & Stevens, R. E. 1938. Taeniolite from Magnet Cove, Arkansas. – Am. Miner. 23: 104–110.

Nash, W. P. & Wilkinson, J. F. G. 1970. Shonkin Sag laccolith, Montana. 1. Mafic minerals and estimates of temperature, pressure, oxygen fugacity and silica activity. – Contr. Miner. Petrol. 25: 241–269.

Neuman, E. R. 1974. The distribution of Mn^{2+} and Fe^{2+} between ilmenites and magnetites in igneous rocks. – Am. J. Sci. 274: 1074–1088.

Neuman, E. R. 1976. Compositional relations among pyroxenes, amphiboles and other mafic phases in the Oslo Region plutonic rocks. – Lithos 9: 85–109.

Nielsen, T. F. D. 1979. The occurrence and formation of Ti-aegirines in peralkaline syenites. An example from the Tertiary ultramafic alkaline Gardiner complex, East Greenland. – Contr. Miner. Petrol. 69: 235–244.

Noe-Nygaard, A. 1941. Syenitforekomsten ved Antarctic Havn (Østgrønland). – Meddr dansk geol. Foren. 9: 550–556.

Noe-Nygaard, A. 1974. Cenozoic to Recent volcanism in and around the North Atlantic basin. – In: Nairn, A. E. M. & Stehli, F. G. (eds). The ocean basins and margins. Vol. 2. – Plenum Publishing, New York: 391–443.

Noe-Nygaard, A. 1976. Tertiary igneous rocks between Shannon and Scoresby Sund, East Greenland. – In: Escher, A. & Watt, W. S. (eds). Geology of Greenland. – The Geological Survey of Greenland, Copenhagen: 386–402.

Pankhurst, R. J., Beckinsale, R. D. & Brooks, C. K. 1976. Strontium and oxygen isotope evidence relating to the petrogenesis of the Kangerdlugssuaq alkaline intrusion, East Greenland. – Contr. Miner. Petrol. 54: 17–42.

Powell, M. & Powell, R. 1977. Plagioclase-alkali feldspar geothermometry revisited. – Contr. Miner. Petrol. 62: 193–204.

Reed, S. J. B. & Ware, N. G. 1975. Quantitative electron microprobe analysis of silicates using energy-dispersive X-ray spectrometry. – J. Petrology 16: 499–519.

Rex, D. C., Gledhill, A. R., Brooks, C. K. & Steenfelt, A. 1979. Radiometric ages of Tertiary salic intrusions near Kong Oscars Fjord, East Greenland. – Rapp. Grønlands geol. Unders. 95: 106–109.

Rock, N. M. S. 1978. Petrology and petrogenesis of the Monchique alkaline complex, southern Portugal. – J. Petrology 19: 171–214.

Rønsbo, J. G., Pedersen, A. K. & Engell, J. 1977. Titan-aegirine from early Tertiary ash layers in northern Denmark. – Lithos 10: 193–204.

Schaub, H. P. 1942. Zur Geologie der Traill Insel (Nordost-Grönland). – Ecolog. geol. Helv. 35 (1): 54 pp.

Segalstad, T. V. & Larsen, A. O. 1978. Chevkinite and perrierite from the Oslo region, Norway. – Am. Miner. 63: 499–505.

Simkin, T. & Smith, J. V. 1970. Minor element distribution in olivine. – J. Geol. 78: 304–325.

Stephenson, D. 1972. Alkali clinopyroxenes from nepheline syenites of the South Qoroq Centre, South Greenland. – Lithos 5: 187–201.

Stern, W. B. 1979. Zur strukturformelberechung von Glimmermineralien. – Schweiz. miner. petrogr. Mitt. 59: 75–82.

Stormer, J. C. Jr. 1975. A practical two feldspar geothermometer. – Am. Miner. 60: 667–674.

Sundius, N. 1945. The composition of eckermannite and its position in the amphibole group. – Årbok Sver. geol. Unders. 39 (8): 1–7.

Thompson, R. N. 1976. Alkali amphiboles in the Eocene, high level granites of Skye, Scotland. – Miner. Mag. 40: 891–893.

Tyler, R. C. & King, B. C. 1967. The pyroxenes of the alkaline igneous complexes of Eastern Uganda. – Miner. Mag. 36: 5–21.

Upton, B. G. J., Macdonald, R., Hill, P. G., Jeffries, B. & Ford, C. E. 1976. Narsarsukite: a new occurrence in peralkaline trachyte, South Greenland. – Miner. Mag. 40: 737–746.

Ussing, N. V. 1912. Geology of the country around Julianehaab. – Meddr Grønland 38: 376 pp.

Vlasov, K. A. 1966. Geochemistry and mineralogy of rare elements and genetic types of their deposits. Vol. II. Mineralogy of rare elements. – Israel Program for Scientific Translations, Jerusalem.

Wager, L. R. 1965. The form and internal structure of the alkaline Kangerdlugssuaq intrusion, East Greenland. – Miner. Mag. 34: 487–497.

Yagi, K. 1966. The system acmite-diopside and its bearing on the stability relations of natural pyroxenes of the acmite-diopside series. – Am. Miner. 51: 976–1000.

Meddelelser om Grønland, Geoscience

1979.

1. C. K. Brooks:
»Geomorphological observations at Kangerdlugssuaq, East Greenland«. 24 pp.

The Kangerdlugssuaq area is mainly comprised of two contrasting rock groups: on the one hand the easily-eroded lavas and sediments of late Mesozoic to early Tertiary age and on the other the highly resistant Precambrian gneisses. Intermediate between these two types in terms of behaviour with respect to erosion are the Tertiary plutonic complexes and the basaltic areas along the coast which have been intruded by intense dyke swarms.

In the late Mesozoic the area was a peneplain, and low relief apparently persisted throughout the volcanic episode as there is good evidence that the lava plateau subsided during its formation. During this period ocean-floor spreading gave rise to the embryonic Danmark Stræde. Shortly after the volcanic episode the Kangerdlugssuaq area became the centre of a massive domal upwarping which has been a dominant feature of the land-forms up to the present day. The original surface of the dome has been reconstructed on the basis of topographic and geological evidence to show that it was elliptical in form with a major axis of at least 300 km in length and a height above present sea-level of about 6.5 km. However, subsequent isostatic effects are not considered in deriving these figures. The updoming is estimated to have occurred about 50 m.y. ago.

Several kilometres thickness of sediments and lavas were eroded off this dome at an early stage exposing the gneissic core, which still stands in alpine peaks up to about 2.7 km altitude in the central part, and dumping ca. 50000 km^3 of sediment on the continental shelf. The erosion was effected by a radial, consequent drainage system, relicts of which can still be found. Kangerdlugssuaq itself may owe its origin to a tectonic line of weakness formed in response to doming, but there are also good arguments for its being purely erosional. The erosion of the dome was probably fluviatile but all trace of this stage has been obliterated by the subsequent glaciation.

In the period between the Eocene and the early Miocene, possibly around 35 m.y. ago, the entire area underwent epeirogenic uplift raising the undeformed parts of the original lava plateau to around 2.5 km above sea-level. At present this plateau is undergoing dissection from the seaward side, but considerable areas are still preserved under thin, horizontal ice-caps.

A brief description of the various types of glaciers, an impermanent, ice-dammed lake and the areas of ice-free land is given. In the Pleistocene, the Kangerdlugssuaq glacier was considerably thicker than at the present time and extended far out over the shelf, excavating a deep channel here. Finally some observations on the coastlines are presented.

1979

2. Sven Karup-Møller and Hans Pauly:
»Galena and associated ore minerals from the cryolite at Ivigtut, South Greenland«. 25 pp.

Silver- and bismuth-rich galena concentrates have been produced for more than 70 years as a byproduct in the dressing of the crude cryolite from Ivigtut, South Greenland.

Concentrates from the years 1937 to 1962 contained from 0.44 % Ag and 0.74 % Bi to 0.94 % Ag and 1.93 % Bi. Conspicuous increases in the content of these elements appeared twice within this time interval, namely in 1955 and in 1960. Thus it seems that crude cryolite from specific areas within the mine carried galena high in silver and bismuth. This promoted a detailed study of the common Ivigtut galena and associated sulphides.

An outline of the geological setting of the deposit is given. The deposit is divided into two main bodies – the cryolite body and the quartz body. Both are subdivided into units characterized by their content of siderite and fluorite. Galena samples from these units and from rock types surrounding the deposit have been studied.

Galena from units characterized by siderite follows the compositional pattern found in the galena concentrates, whereas the sparse galena mineralizations from units characterized by fluorite contain much smaller amounts of silver and bismuth, less than 0.2 %. However, within the fluorite-bearing units, two peculiar parageneses reveal high contents of silver and bismuth expressed by the presence of particular minerals such as matildite-aikinite and gustavite-cosalite respectively.

Further trace element studies on selected galena samples emphasize Sn and Te as chemically characteristic of the galena and of the sulphide-carbonate phase of the deposit.

The temperature of formation of the main part of the deposit is placed at 550–400°C, and between 300 and 200°C for certain parts of the fluorite cryolite and the fluorite zone.

1980

3. John C. Rucklidge, Charles Kent Brooks and Troels F. D. Nielsen: »Petrology of the coastal dykes at Tugtilik, southern East Greenland«. 17 pp.

Dolerite and lamprophyre dikes from Tugtilik in the southern part of the onshore exposure of the East Greenland coastal dike swarm are described. The dolerites, which are earlier, are similar to other tholeiites from the dike swarm and the plateau basalts and also to many Icelandic tholeiites. Transitional varieties have been identified from the Angmagssalik district. The lamprophyres have a nephelinitic composition and are rich in phenocrysts and xenocrysts. In one case, abundant low pressure inclusions occur. Rocks identical to these lamprophyres have not previously been described from Greenland but are well known, for instance, in the African Rift.

1981

4. Barbara H. Scott: »Kimberlite and lamproite dykes from Holsteinsborg, West Greenland«. 24 pp.

Numerous kimberlite and lamproite dykes occur to the south and east of Holsteinsborg in Central West Greenland. This paper gives details of the petrography, mineral chemistry, age relations and geochemistry of the dykes.

The kimberlites are composed of macrocysts of olivine, phlogopite, rare ilmenite and garnet in a matrix of olivine, phlogopite, diopside perovskite, spinel, serpentine, carbonate and apatite. They can mostly be classified as clinopyroxene-phlogopite hypabyssal kimberlites. Mantle-derived inclusions are found in some of the dykes and include lherzolites, wehrlites, harzburgites and, most commonly, dunites. Both coarse and porphyroclastic inclusions occur. Garnet-granulites and eclogites, although rare, are present.

The lamproites have variable mineral assemblages and textures but the main constituents are phenocrysts of pseudoleucite, olivine, phlogopite and clinopyroxene set in a groundmass of phlogopite, potassic richterite, diopside, pseudoleucite and potassium feldspar. The mineralogy of these dykes is a reflection of unusual ultrapotassic, magnesian whole-rock compositions.

1981

5. Svante Björck and Thomas Persson: »Late Weichselian and Flandrian biostratigraphy and chronology from Hochstetter Forland, Northeast Greenland«. 19 pp.

Two lakes on Hochstetter Forland have been analysed with respect to lithostratigraphy and pollen and algae stratigraphy. The sediments have been radiocarbon dated and these dates show that Hochstetter Forland was not covered by the Inland Ice during the Late Weichselian. The early Flandrian stratigraphic sequences of the two lakes are interrupted by barren interzones, dated at 10 100 – 8100 B. P. and 10 100 – 9200 B. P., which are partly correlated to an ice-advance. No evidence for an earlier ice-advance during the Late Weichselian has been found. Apart from the abundance of pollen grains indicating pioneer vegetation, *Artemisia* pollen grains are found in high quantities in the Late Weichselian, although it is today not found within the area. The Flandrian pollen stratigraphy indicates a development similar to that which has been found in the Scoresby Sund area. However, *Cassiope tetragona* and *Salix arctica* immigrate much earlier than further south. The Flandrian climatic optimum in the Hochstetter Forland area seems to have been reached between 6000 and 5000 B. P. The Flandrian shore-line displacement is roughly estimated.

1981

6. T. F. D. Nielsen, N. J. Soper, C. K. Brooks, A. M. Faller, A. C. Higgins and D. W. Matthews:
»The pre-basaltic sediments and the Lower Basalts at Kangerdlugssuaq, East Greenland: their stratigraphy, lithology, palaeomagnetism and petrology«. 25 pp.

This paper presents a new 1:40 000 topographic and geological map of the area around Miki Fjord and I. C. Jacobsen Fjord, East Greenland. The post-Precambrian sedimentary succession, the Kangerdlugssuaq Group, begins with the Ryberg Formation (Campanian to Danian (?)) and continues into the Vandfaldsdalen Formation of Late Paleocene age. These sediments were laid down in a basin which subsequently became filled and covered by basaltic rocks of the Blosseville Group, including lavas, hyaloclastites, tuffs and breccias. Considerable facies variations are apparent in both the sediments and volcanics indicating that the basin deepened in an easterly direction. Palaeomagnetic measurements confirm previous results for the Blosseville Group on the Lower Basalts but do not yet entirely eliminate the possibility that some of the succession has normal polarity. Petrographically the volcanics include picrites (oceanites and ankaramites), olivine tholeiites, tholeiites and tholeiitic andesites. They have almost all suffered alteration up to greenschist facies and some show evidence of sedimentary contamination. They are all of tholeiitic affinity and are Fe and Ti enriched when compared to normal ocean ridge basalts. They are however much more variable in composition than the overlying Plateau Basalts and have not been produced in such large volumes. It is suggested that a primary picritic magma gave rise to the oceanites and ankaramites by olivine and clinopyroxene fractionation and accumulation. The olivine tholeiites, which appear to be separated from the picrites by a compositional gap, may be derived from a different parental magma. Petrological parallels are drawn with other provinces.

Instructions to authors

Manuscripts will be forwarded to referees for evaluation. Authors will be notified as quickly as possible about acceptance, rejection, or desired alterations. The final decision rests with the editor. Authors receive two page proofs. Prompt return to the editor is requested.

Alterations against the ms. will be charged to the author(s). Twenty five offprints are supplied free. Order form, quoting price, for additional copies accompanies 2nd proof. Manuscripts (including illustrations) are not returned to the author(s) after printing unless especially requested.

Manuscript

General. – Manuscripts corresponding to less than 16 printed pages (of 6100 type units) incl. illustrations, are not accepted. Two copies of the ms. (original and one good quality copy), each complete with illustrations should be sent to the Secretary.

All Greenland placenames in text and illustrations must be those authorized. Therefore sketch-maps with all the required names should be forwarded to the Secretary for checking before the ms. is submitted.

Language. – Manuscripts should be in English (preferred language), French, or German. When appropriate the language of the ms. must be revised before submission.

Title. – Titles should be kept as short as possible and with emphasis on words useful for indexing and information retrieval.

Abstract. – An English abstract should accompany the ms. It should be short, outline main features, and stress novel information and conclusions.

Typescript. – Page 1 should contain: (1) title, (2) name(s) of author(s), (3) abstract, and (4) author's full postal address(es). Large mss. should be accompanied by a Table of Contents, typed on separate sheet(s). The text should start on p. 2. Consult a recent issue of the series for general lay-out.

Double space throughout and leave a 4 cm left margin. Footnotes should be avoided. Desired position of illustrations and tables should be indicated with pencil in left margin.

Underlining should only be used in generic and species names. The use of italics in other connections is indicated by wavy line in pencil under appropriate words. The editor undertakes all other type selection.

Use three or fewer grades of headings, but do not underline. Avoid long headings.

References. – Reference to figures and tables in the text should have this form: Fig 1; Figs 2–4, Table 3. Bibliographic references in the text are given as: Shergold (1975: 16) and (Jago & Daily 1974b).

In the list of references the following usage is adopted:

Journal: Tarling, D. H. 1967. The palaeomagnetic properties of some Tertiary lavas from East Greenland. – Earth planet. Sci. Lett. 3: 81–88.

Book: Boucot, A. J. 1975. Evolution and extinction rate controls. – Elsevier, Amsterdam: 427 pp.

Chapter (part): Wolfe, J. A. & Hopkins, D. M. 1967. Climatic changes recorded by Tertiary landfloras in northwestern North America. – In: Hatai, K. (ed.), Tertiary correlations and climatic changes in the Pacific. – 11th Pacific Sci. Congr. Tokyo 1966, Symp.: 67–76.

Title of journals should be abbreviated according to the last (4th) edition of the World List of Scientific Periodicals (1960) and supplementary lists issued by BUCOP (British Union-Catalogue of Periodicals). If in doubt, give the title in full.

Meddelelser om Grønland, Geoscience should be registered under *Meddelelser om Grønland.* Example (with authorized abbreviations): *Meddr Grønland, Geosci.* 1, 1979.

Illustrations

General. – Submit two copies of each graph, map, photograph, etc., all marked with number and author's name. Normally all illustrations will be placed within the text; this also applies to composite figures.

All figures (incl. line drawings) must be submitted as glossy photographic prints suitable for direct reproduction, i.e. having the format of the final figure. Do not submit original artwork. Where appropriate the scale should be indicated in the caption or in the illustration.

The size of the smallest letters in illustrations should not be less than 1.5 mm. Intricate tables are often more easily reproduced from line drawings than by type-setting.

Colour plates may be included at the author's expense, but the editor should be consulted before such illustrations are submitted.

Size. – The width of figures must be that of a column (77 mm) 1½ column (117 mm) or of a page (157 mm). Remember to allow space for captions below full page figures. Maximum height of figures (incl. captions) is 217 mm. Horizontal figures are preferred.

If at all possible, fold-out figures and tables should be avoided.

Caption. – Caption (two copies) to figures should be typed on separate sheets.

Meddelelser om Grønland

Geoscience 7 · 1982

Meddelelser om Grønland

Bioscience
Geoscience
Man & Society

Published by
The Commission
for Scientific
Research
in Greenland

1982

AIO Print as, Odense, Denmark